AMERICAN SOCIETY FOR MICROBIOLOGY | mBio

Check for updates

| Microbial Ecology | Research Article

Production and cross-feeding of nitrite within *Prochlorococcus* populations

Paul M. Berube,[1] Tyler J. O'Keefe,[1] Anna Rasmussen,[1] Trent LeMaster,[1] Sallie W. Chisholm[1,2]

AUTHOR AFFILIATIONS See affiliation list on p. 14.

ABSTRACT *Prochlorococcus* is an abundant photosynthetic bacterium in the open ocean, where nitrogen (N) often limits phytoplankton growth. In the low-light-adapted LLI clade of *Prochlorococcus*, nearly all cells can assimilate nitrite (NO_2^-), with a subset capable of assimilating nitrate (NO_3^-). LLI cells are maximally abundant near the primary NO_2^- maximum layer, an oceanographic feature that may, in part, be due to incomplete assimilatory NO_3^- reduction and subsequent NO_2^- release by phytoplankton. We hypothesized that some *Prochlorococcus* exhibit incomplete assimilatory NO_3^- reduction and examined NO_2^- accumulation in cultures of three *Prochlorococcus* strains (MIT0915, MIT0917, and SB) and two *Synechococcus* strains (WH8102 and WH7803). Only MIT0917 and SB accumulated external NO_2^- during growth on NO_3^-. Approximately 20–30% of the NO_3^- transported into the cell by MIT0917 was released as NO_2^-, with the rest assimilated into biomass. We further observed that co-cultures using NO_3^- as the sole N source could be established for MIT0917 and *Prochlorococcus* strain MIT1214 that can assimilate NO_2^- but not NO_3^-. In these co-cultures, the NO_2^- released by MIT0917 is efficiently consumed by its partner strain, MIT1214. Our findings highlight the potential for emergent metabolic partnerships that are mediated by the production and consumption of N cycle intermediates within *Prochlorococcus* populations.

IMPORTANCE Earth's biogeochemical cycles are substantially driven by microorganisms and their interactions. Given that N often limits marine photosynthesis, we investigated the potential for N cross-feeding within populations of *Prochlorococcus*, the numerically dominant photosynthetic cell in the subtropical open ocean. In laboratory cultures, some *Prochlorococcus* cells release extracellular NO_2^- during growth on NO_3^-. In the wild, *Prochlorococcus* populations are composed of multiple functional types, including those that cannot use NO_3^- but can still assimilate NO_2^-. We show that metabolic dependencies arise when *Prochlorococcus* strains with complementary NO_2^- production and consumption phenotypes are grown together on NO_3^-. These findings demonstrate the potential for emergent metabolic partnerships, possibly modulating ocean nutrient gradients, that are mediated by cross-feeding of N cycle intermediates.

KEYWORDS *Prochlorococcus*, *Synechococcus*, primary nitrite maximum, nitrogen cycle, cross-feeding

Prochlorococcus and its close relative, *Synechococcus*, are globally abundant non-diazotrophic cyanobacteria that are jointly responsible for approximately 25% of marine net primary production (1). Phytoplankton growth, and thus primary production, is limited by N across much of the surface ocean (2). Given the numerical dominance of *Prochlorococcus*, examining its genotypic and phenotypic diversity in the context of the N cycle can inform our understanding of *Prochlorococcus'* role in marine ecosystems.

Prochlorococcus has multiple N assimilation traits, most of which are distributed across cells in *Prochlorococcus* populations. All *Prochlorococcus* appear capable of

Editor Nicole Dubilier, Max Planck Institute for Marine Microbiology, Bremen, Germany

Address correspondence to Paul M. Berube, pmberube@mit.edu.

The authors declare no conflict of interest.

See the funding table on p. 14.

Received 16 May 2023
Accepted 23 May 2023
Published 5 July 2023

assimilating ammonium (NH_4^+), which is a preferred N source for cyanobacteria likely because it requires less reducing power to assimilate compared to more oxidized N sources (3). Some, but not all, *Prochlorococcus* possess genes enabling the assimilation of urea, cyanate, amino acids, NO_2^-, and NO_3^- (4–10). It is now evident that there is extensive variability with respect to the N assimilation traits harbored by *Prochlorococcus*. These biological features have the potential to impact N cycling across the vast subtropical ocean gyres—the consequences of which are not well constrained.

The evolutionary history of NO_3^- assimilation in *Prochlorococcus* has deepened our understanding of the selective pressures operating on this organism. Among low-light-adapted *Prochlorococcus*, only the LLI clade has retained the genes for NO_3^- assimilation, while this trait is found in many high-light-adapted clades—e.g., HLI, HLII, and HLVI (10). High-light-adapted cells with NO_3^- assimilation genes appear to be selected for in the surface waters of N-limited systems (9). In contrast, selection for LLI *Prochlorococcus* cells with the capacity to assimilate NO_3^- is not well resolved. This group of *Prochlorococcus* is widely distributed and abundant, often exceeding the combined depth-integrated abundance of other low-light-adapted *Prochlorococcus* (11, 12). Intriguingly, we observed a spatial relationship between LLI cells with the NO_3^- assimilation trait and a peak in NO_2^- concentration in the water column (9).

In stratified marine systems, elevated concentrations of NO_2^- in the mid-euphotic zone are ubiquitous. This feature, the primary NO_2^- maximum layer, is thought to arise from distinct biological processes—either decoupled nitrification (13–16) or incomplete NO_3^- reduction by phytoplankton (14, 17). Phytoplankton can be subject to multiple factors affecting the degree to which they excrete NO_2^- during growth on NO_3^- (18). These factors include light (19), growth rate (20), temperature (21), external NO_3^- concentration (22–24), Fe limitation (25), and N deficiency (22, 26).

Several features of *Prochlorococcus*' diversity suggest that NO_2^- cycling could be an important facet of this organism's ecology, particularly for the abundant low-light-adapted LLI clade of *Prochlorococcus* that dominates the upper reaches of the nitracline. Among these *Prochlorococcus*, the NO_2^- assimilation trait appears to be found in most or all cells while the full pathway for NO_3^- assimilation is only observed in a subset of cells (10). These trait frequencies bear the hallmarks of medium-frequency-dependent selection, which are often governed by cross-feeding interactions (27). Given that LLI *Prochlorococcus* live in the vicinity of the primary NO_2^- maximum layer, we hypothesized that those capable of NO_3^- assimilation have the potential for releasing NO_2^- back into the environment—consistent with what is observed in larger size classes of phytoplankton (18). In this study, we explore incomplete assimilatory NO_3^- reduction by *Prochlorococcus* and further examine the potential for cross-feeding and intra-population cycling of NO_2^-, a central intermediate in the N cycle.

RESULTS AND DISCUSSION

Prochlorococcus strains produce NO_2^- during growth on NO_3^-

We first asked whether *Prochlorococcus*, as well as closely related *Synechococcus*, exhibit incomplete assimilatory NO_3^- reduction with concomitant NO_2^- release (18). To address this question, we leveraged a collection of strains (Table S1) with different gene contents (Table S2) and configurations of the NO_3^- and NO_2^- assimilation gene cassette (10). We looked for evidence of extracellular accumulation of NO_2^- during the growth of *Prochlorococcus* and *Synechococcus* strains on NO_3^- in comparison to growth on NH_4^+ as the sole N sources. Given that reducing power is ultimately derived from photochemistry in cyanobacteria, we also tested if extracellular accumulation of NO_2^- might be enhanced during growth at lower light intensities—e.g., the reduction of NO_3^- to NO_2^- requires two electrons, while the reduction of NO_2^- to NH_4^+ requires six electrons, contributing to a possible bottleneck under light limitation.

For cultures of *Prochlorococcus* MIT0915, we found that NO_2^- concentrations remained below 1 µM (the lower limit of the dynamic range for our assay) at all examined light intensities during growth on NO_3^- (Fig. 1). For the closely related MIT0917 strain,

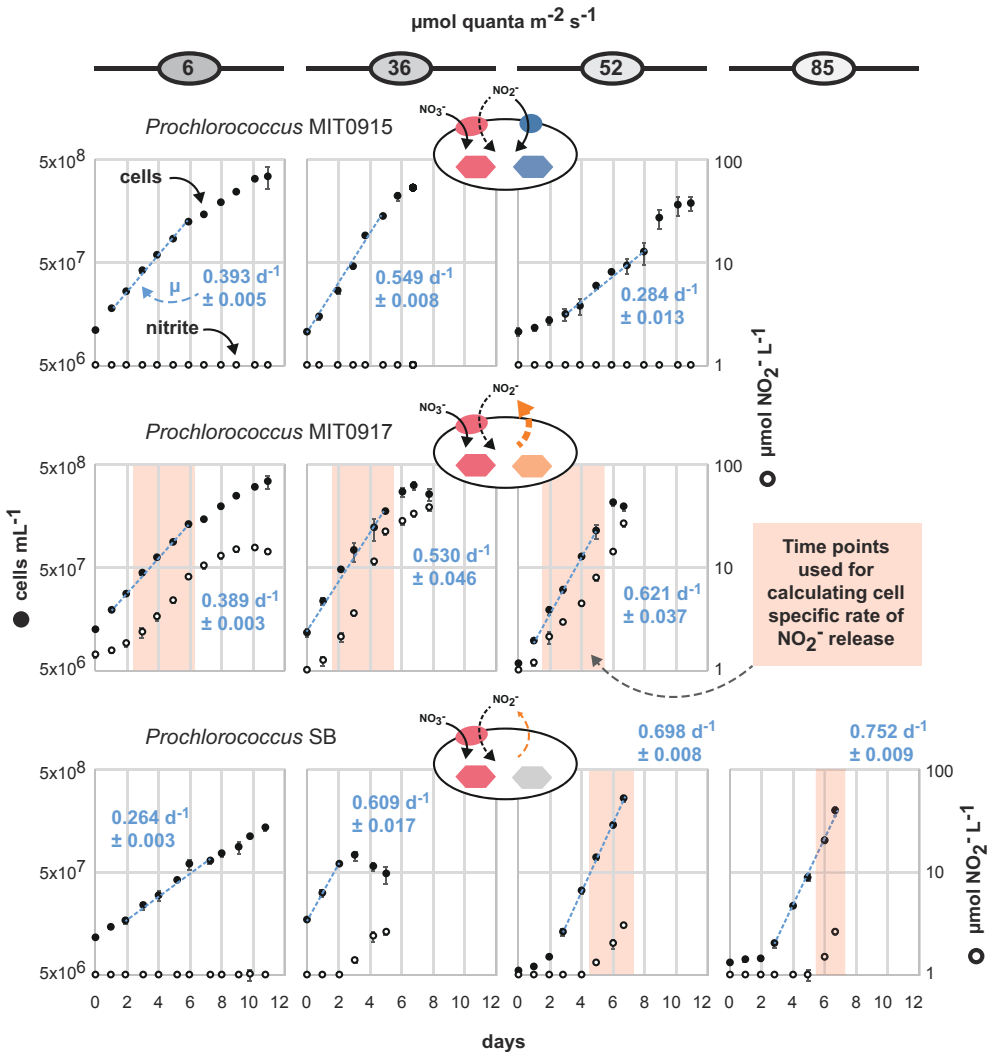

FIG 1 NO_2^- accumulation in triplicate batch cultures of *Prochlorococcus* during growth on NO_3^- as the sole N source over a range of light intensities. Mean cell concentrations are denoted by closed black circles with error bars representing standard deviations. Growth rates (mean and standard deviation of µ for each replicate culture) are shown as blue text with the regression shown as a dashed blue line inclusive of the data points used to calculate growth rates. Mean NO_2^- concentrations are denoted by open circles with error bars representing standard deviations. NO_2^- concentrations below the dynamic range of the assay (<1 µM NO_2^-) are plotted on the *x*-axis. Cell-specific rates of NO_2^- release (nmol NO_2^- $cell^{-1}$ d^{-1}) were calculated from the log-linear portion of the growth curve (inclusive data points are indicated by red shading).

cultures accumulated substantial concentrations of NO_2^- when provided NO_3^- as the sole N source (Fig. 1) compared to growth on NH_4^+ (Fig. S1). The high-light-adapted *Prochlorococcus* SB accumulated NO_2^- in the culture medium during growth on NO_3^- but at substantially lower concentrations and with a noticeably greater lag compared to MIT0917 (Fig. 1). In comparison to the *Prochlorococcus* strains examined, neither of the *Synechococcus* strains produced levels of NO_2^- that exceeded 1 µM during growth on NO_3^- or NH_4^+ (Fig. 2; Fig. S2).

We next examined the net cell-specific NO_2^- production rates of MIT0917 and SB during growth on NO_3^-. The rates of NO_2^- excretion by the low-light-adapted *Prochlorococcus* MIT0917 were significantly greater than that for the high-light-adapted *Prochlorococcus* SB (Fig. 3). At the same light intensity of 52 µmol photons m^{-2} s^{-1}, MIT0917 produced NO_2^- at a fivefold higher rate compared to SB (Fig. 3). The rate of NO_2^- production by MIT0917 was higher at 36 and 52 µmol photons m^{-2} s^{-1} in comparison to the lowest light intensity examined. These rates are necessarily inclusive of potential

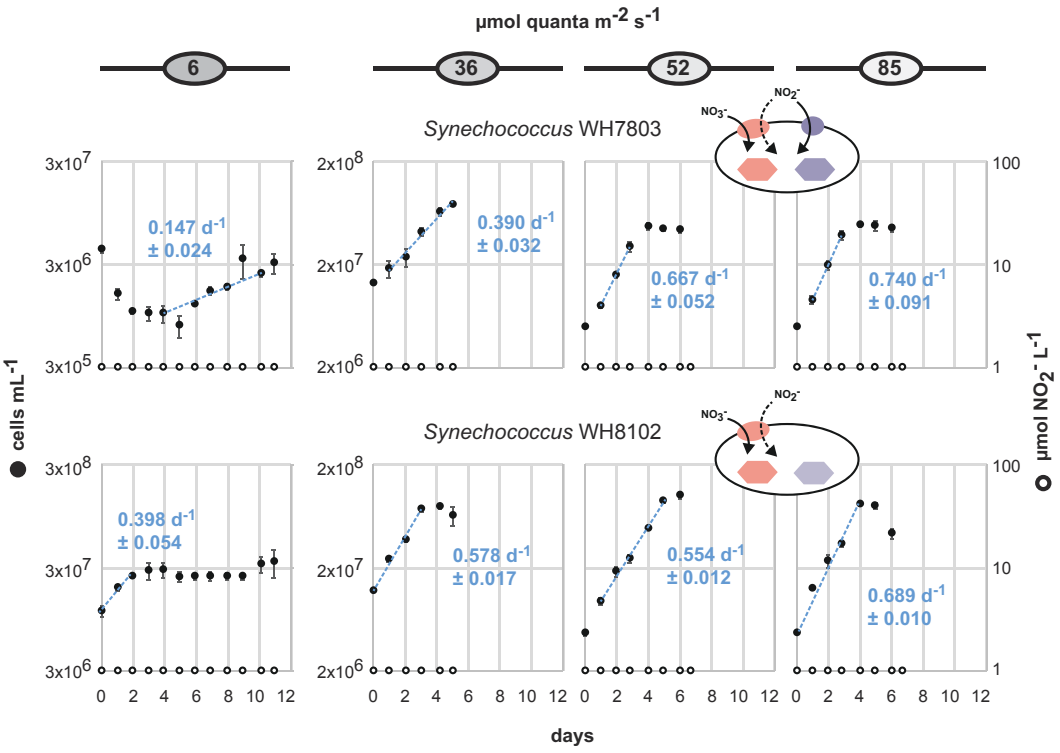

FIG 2 NO_2^- accumulation in triplicate batch cultures of *Synechococcus* during growth on NO_3^- as the sole N source over a range of light intensities. Mean cell concentrations are denoted by closed black circles with error bars representing standard deviations. Growth rates (mean and standard deviation of µ for each replicate culture) are shown as blue text with the regression shown as a dashed blue line inclusive of the data points used to calculate growth rates. Note that the cell concentration range (left *y*-axis) on the plots for cultures grown at 6 µmol photons m^{-2} s^{-1} differs from the plots of cultures grown at higher light intensities. Mean NO_2^- concentrations are denoted by open circles with error bars representing standard deviations. NO_2^- concentrations below the dynamic range of the assay (<1 µM NO_2^-) are plotted on the *x*-axis.

reuptake of NO_2^- by the NapA transporter encoded by both MIT0917 and SB. NapA has been shown to transport both NO_3^- and NO_2^- in other cyanobacteria (28). Nevertheless, reuptake of NO_2^- could be limited by the fact that the molar equivalents of NO_3^- would exceed that of NO_2^- by at least one order of magnitude throughout the entire growth curve and because of preferential transport of NO_3^- over NO_2^- by NapA as observed for other cyanobacteria (28).

The rates of NO_2^- release we observed for MIT0917 (from 2.4×10^{-8} to 6.6×10^{-8} nmol NO_2^- $cell^{-1}$ d^{-1}) are consistent with rates measured for marine diatoms when normalized to either C quotas (as a proxy for biomass) or cell volumes. In batch culture experiments, *Thalassiosira pseudonana* was observed to produce NO_2^- during growth on NO_3^- at a maximum rate of 2.5×10^{-14} µmol s^{-1} $cell^{-1}$ (2.2×10^{-6} nmol NO_2^- $cell^{-1}$ d^{-1}) (29). Note that diatoms are much larger than cyanobacteria: *T. pseudonana* was observed to have a C quota of 14,000 fg $cell^{-1}$ and a cell volume of 46 $µm^{-3}$ (30), while LLI *Prochlorococcus* were reported to have a C quota of 33 fg $cell^{-1}$ and a cell volume of 0.14 $µm^{-3}$ (31). Thus, *T. pseudonana* cells have approximately 420-fold greater biomass and a 330-fold larger cell volume than LLI *Prochlorococcus* cells. When these ratios in biomass or cell volume are accounted for, MIT0917 produced NO_2^- at normalized rates over threefold higher than *T. pseudonana*.

We then wondered how consequential these rates of NO_2^- release by MIT0917 were with respect to the N requirements of low-light-adapted *Prochlorococcus*. To evaluate this question, we assumed a cellular N quota of 4.3 fg N $cell^{-1}$ for LLI *Prochlorococcus* (31), minimal reuptake of NO_2^-, and minimal excretion of other N containing compounds. Based on these assumptions, we estimate that approximately 20–30% of the NO_3^- transported into the cell by MIT0917 during exponential growth may be released as

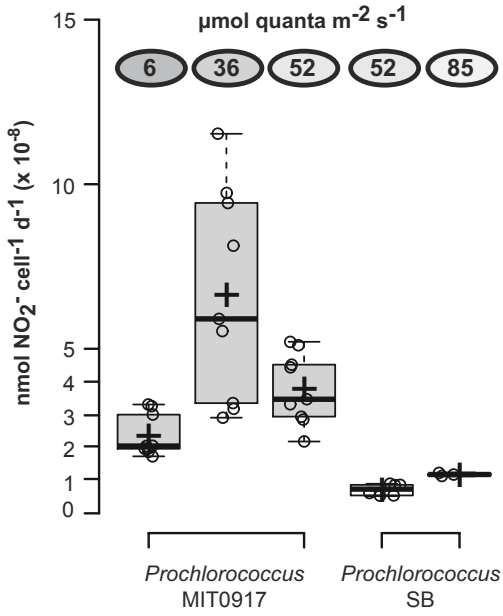

FIG 3 Cell-specific NO_2^- production rates for two strains of *Prochlorococcus*, as a function of light intensity, when grown on NO_3^- as the sole N source. Cell-specific NO_2^- production rates were calculated as the change in NO_2^- concentration relative to the logarithmic mean of cell concentrations—to account for exponential growth—for successive time points during the log-linear portion of the growth curve. Each open circle represents the net cell-specific NO_2^- accumulation rate calculated from a pair of successive time points during exponential growth—inclusive time points are shown in Fig. 1. Means are denoted by crosses, and medians are denoted by solid black lines. The means (± standard deviation) of NO_2^- production rates for MIT0917 were 2.4×10^{-8} ($\pm 0.64 \times 10^{-8}$), 6.6×10^{-8} ($\pm 3.2 \times 10^{-8}$), and 3.8×10^{-8} ($\pm 1.1 \times 10^{-8}$) nmol NO_2^- cell^{-1} d^{-1} at light intensities of 6, 36, and 52 µmol photons m^{-2} s^{-1}, respectively. SB produced nitrite at rates of 7.2×10^{-9} ($\pm 1.7 \times 10^{-9}$) and 1.2×10^{-8} ($\pm 0.05 \times 10^{-8}$) nmol NO_2^- cell^{-1} d^{-1} at light intensities of 52 and 85 µmol photons m^{-2} s^{-1}, respectively. Medians are denoted by solid black lines, and means are denoted by crosses.

NO_2^-, with the balance assimilated into biomass (i.e., the proportion of N as extracellular NO_2^- relative to the combined N in both biomass and extracellular NO_2^-). While a broad range of NO_2^- excretion to NO_3^- uptake ratios have been observed previously (18), our estimate for MIT0917 is consistent with values obtained for other phytoplankton (18).

Overall, these data demonstrate that some strains belonging to an abundant low-light-adapted clade of *Prochlorococcus* can release high amounts of NO_2^- when provided NO_3^- as the sole N source. Even high-light-adapted *Prochlorococcus* may release meaningful amounts of NO_2^- when growing on NO_3^-. Importantly, the generally positive relationship between light intensity and NO_2^- production rates for both MIT0917 and SB argues against the hypothesis of enhanced NO_2^- release at lower light intensities. To assess alternatives, we looked to the genetic repertoire of these strains as well as the distribution of NO_3^- and NO_2^- assimilating genotypes of LLI *Prochlorococcus* in the wild.

Contrasting features of NO_3^- and NO_2^- flow in *Prochlorococcus* and *Synechococcus*

Based on what is known about the gene content (Table S2) and physiology (Fig. 1 and 2) of these strains, we can assign hypothetical pathways of inorganic N flow (Fig. 4). For LLI *Prochlorococcus*, these hypothetical pathways map onto the three distinct configurations of the NO_3^- and NO_2^- assimilation gene cassette that we have observed in their genomes (10). Many LLI *Prochlorococcus* have the configuration represented by MIT1214—i.e., they can assimilate both NH_4^+ and NO_2^- but not NO_3^-. The remaining LLI *Prochlorococcus*—those represented by the NO_3^- assimilating strains, MIT0915 and

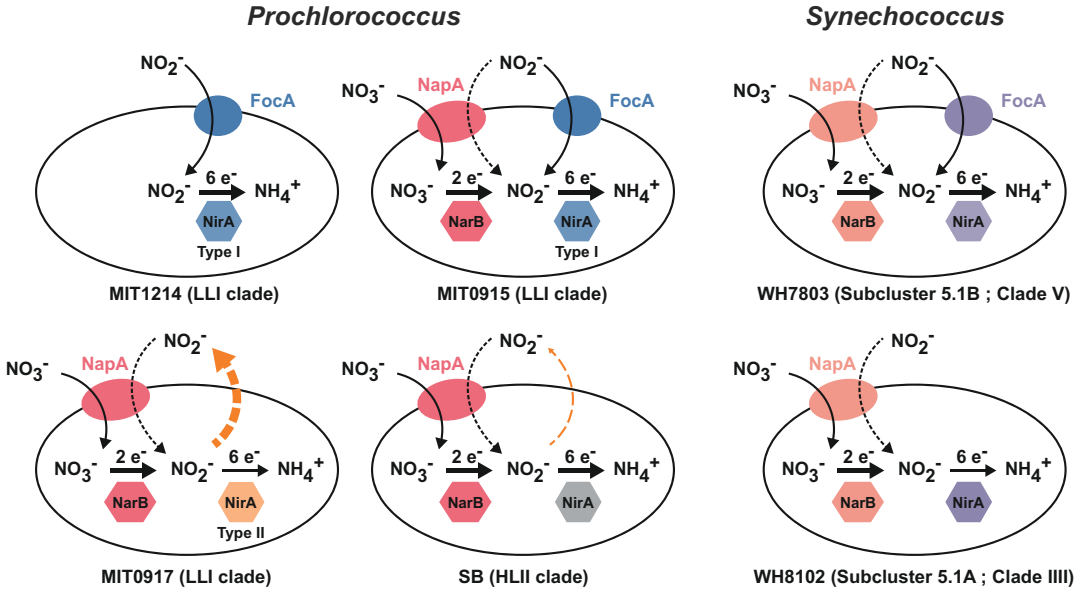

FIG 4 Schematic of cellular inorganic N inputs and outputs for *Prochlorococcus* and *Synechococcus* strains based on physiology data (Fig. 1 and 2) and the genetic inventory of NO_3^- and NO_2^- assimilation genes in their genomes (Table S2). MIT1214 has lost the upstream half of the NO_3^- assimilation pathway but has retained FocA and the type I NirA for the transport and assimilation of NO_2^-. MIT0915 has a type I NirA and has also retained the FocA NO_2^- transporter—MIT0915 did not excrete NO_2^- during growth on NO_3^- (Fig. 1). MIT0917 has an alternate version of NirA (type II) compared to other LLI strains and lacks the FocA NO_2^- transporter. SB lacks a dedicated NO_2^- transporter (FocA) but can likely take up NO_2^- using the putatively dual-specific NO_3^-/NO_2^- NapA transporter. Both SB and MIT0917 excrete NO_2^- (dashed orange arrow). In comparison to the *Prochlorococcus* strains examined, neither *Synechococcus* strain releases NO_2^- during growth on NO_3^- (Fig. 2). WH7803 possesses the FocA NO_2^- transporter, while WH8102 does not.

MIT0917—have contrasting features with regard to NO_2^- production potential (Fig. 4). Under the N-replete conditions we examined, MIT0917 accumulated high extracellular quantities of NO_2^- relative to the proportion of N that was ultimately assimilated into biomass. The closely related MIT0915 strain, however, released negligible quantities of NO_2^- under the same conditions. Besides the absence of a FocA NO_2^- transporter in MIT0917, one key difference between MIT0917 and MIT0915 is the presence of a distinct NirA nitrite reductase in MIT0917 (Fig. 4). Found in other LLI *Prochlorococcus* genomes, this "type II" NirA is phylogenetically divergent from the NirA possessed by MIT1214 and MIT0915 (10). Thus, N transport and reduction kinetics are implicated in the physiological basis for nitrite release by some *Prochlorococcus*.

Prochlorococcus SB produced much less NO_2^- during growth on NO_3^- than *Prochlorococcus* MIT0917—and only at the highest light intensities examined—but, similar to MIT0917, SB also lacks the FocA NO_2^- transporter (Fig. 4). *Prochlorococcus* SB belongs to the high-light-adapted HLII clade, which is the most abundant clade of *Prochlorococcus* globally and can represent >90% of depth-integrated *Prochlorococcus* in warm tropical and subtropical waters (12). Although the culturing conditions we employed are quite different than those that cells experience in the wild, HLII clade cells with the potential for NO_2^- release—even if less than that of some LLI clade cells—could have an important impact on NO_2^- cycling in the global ocean due to their sheer abundance. *Synechococcus*, while broadly distributed and responsible for a greater fraction of net primary production compared to *Prochlorococcus*, does not appear to release NO_2^- in batch culture (Fig. 2 and 4). One notable observation is that *Synechococcus* WH8102, like the *Prochlorococcus* strains MIT0917 and SB, lacks the FocA NO_2^- transporter (Table S2), yet unlike the *Prochlorococcus* strains, does not accumulate extracellular NO_2^- (Fig. 2). Given that WH8102 did not release NO_2^-, even at the lowest light intensities, we suspect this strain's phenotype may be imparted by the biochemical features of its NapA transporter and/or NO_3^- and NO_2^- reductases that had evolved under different

ecological constraints. Regardless, an important caveat is that the strains we examined represent only a fraction of the diversity of *Synechococcus*.

Wild populations of LLI clade *Prochlorococcus* comprised coexisting functional types delineated by their use of NO_3^- and NO_2^-

In both the subtropical North Pacific and North Atlantic oceans, LLI *Prochlorococcus* (either with or without the capacity for NO_3^- assimilation) often reach maximum abundance within the subsurface chlorophyll maximum layer (12) and in the vicinity of the primary NO_2^- maximum layer (9). Our data now indicate that there is a significant degree of phenotypic diversity with respect to the use of NO_2^- and NO_3^- and that this functional diversity maps onto the genomic diversity of the LLI clade of *Prochlorococcus*. Given these observations, how are LLI *Prochlorococcus* populations structured with respect to the three distinct functional types that we have identified (Fig. 4)? To address this question, we turned to metagenomic data (32) derived from samples collected over 2 years (2003–2004) from the subsurface chlorophyll maximum layer at time-series stations in the North Pacific Subtropical Gyre (Hawai'i Ocean Time-series; HOT) and the North Atlantic Subtropical Gyre (Bermuda Atlantic Time-series Study; BATS). We assessed the frequencies of the *narB, focA*, and both types of the *nirA* gene relative to the *gyrB* gene (a single copy core gene encoding DNA gyrase subunit B) to estimate the fraction of cells in LLI populations that possessed each version of the nitrate assimilation gene cluster (Supplementary Materials and Methods).

At both sites, we observed that MIT1214-like cells (those that assimilate NO_2^- but not NO_3^-) dominated the LLI *Prochlorococcus* populations throughout the year and generally exceeded 60% of total LLI genomes (Fig. 5). At HOT in the North Pacific, overall frequencies of each functional type were quite stable on seasonal time scales, with each of the NO_3^- assimilating functional types making up roughly 15% of the population (Fig. 5). In contrast, the seasonal dynamics at BATS in the North Atlantic were readily apparent for the MIT0917-like functional type which waned in the winter and spring and then increased in the summer (Fig. 5). These observations are consistent with previous work that demonstrated higher abundances of HLII *Prochlorococcus* with the potential for NO_3^- assimilation during the summer and autumn in the North Atlantic (9), when overall

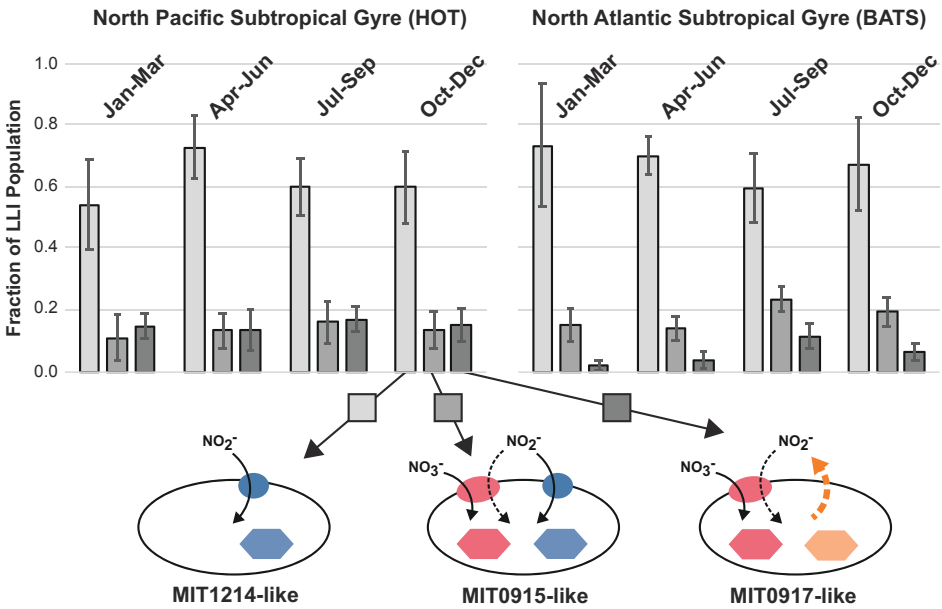

FIG 5 Distribution of functional types in the LLI clade *Prochlorococcus* (based on N flow pathways in Fig. 4) in the North Pacific (HOT) and North Atlantic (BATS) subtropical gyres. Error bars represent the standard deviation of samples grouped by season collected between January 2003 and December 2004. Sample numbers (N) were 6, 6, 4, and 6 at HOT and 5, 5, 4, and 6 at BATS for winter, spring, summer, and autumn, respectively.

surface N concentrations were low. The MIT0915-like functional type (the one that did not exhibit incomplete assimilatory NO_3^- reduction in our culture experiments) generally dominated the NO_3^- assimilating functional types in LLI *Prochlorococcus* populations at the North Atlantic's BATS station (Fig. 5). In contrast, higher frequencies of the MIT0917-like functional type (the one that releases NO_2^-) in the North Pacific compared to the North Atlantic suggest that the configuration of the NO_3^- assimilation gene cassette encoding a type II NirA provides a selective advantage to cells in the stable, well-stratified, and generally N-limited waters of the North Pacific Subtropical Gyre.

Prochlorococcus exchange N in co-cultures

Given that LLI *Prochlorococcus* with different N assimilation features (Fig. 4) coexist in the marine environment (Fig. 5), we next assessed whether strains with different N assimilation genotypes could form metabolic dependencies in the laboratory. To achieve this, we co-cultured *Prochlorococcus* MIT1214 (which can use NO_2^- but not NO_3^-) with either *Prochlorococcus* MIT0915 or *Prochlorococcus* MIT0917 (each of which can use both NO_3^- and NO_2^-) in medium containing NO_3^- as the sole N source.

Pure cultures of MIT0917 grown at 16 µmol photons m^{-2} s^{-1} of blue light produced nitrite at rates from 4.6×10^{-8} to 5.4×10^{-8} nmol NO_2^- $cell^{-1}$ d^{-1} (Fig. 6B and F). These rates are between those observed for MIT0917 grown at 6 and 36 µmol photons m^{-2} s^{-1} of white light (Fig. 1 and 3), suggesting that light spectra may have little impact on nitrite production rates. Relative to these pure cultures of MIT0917 (Fig. 6B and F), co-cultures of MIT1214 and MIT0917 did not accumulate NO_2^- in the culture medium during balanced exponential growth (Fig. 7A and B) because any NO_2^- released by MIT0917 was used to fulfill the N requirements of MIT1214. Some NO_2^- accumulation was observed as the MIT1214-MIT0917 co-culture approached stationary phase (Fig. 7A and B), suggesting an imbalance between production and consumption of NO_2^- outside of balanced exponential growth. The growth rates of each of the two strains in co-culture (Fig. 7C and D) were similar to their growth rates in pure culture (Fig. 6B and D), suggesting that MIT0917 could supply nearly all of the N needs of MIT1214. Furthermore, we expect that the growth of MIT1214 under these conditions resembles growth in continuous culture systems—i.e., in co-culture, MIT1214 was likely poised at some degree of N limitation with growth controlled by the rate of NO_2^- release by the partner strain. Although MIT1214 started at a higher cell density than MIT0917, the frequency of the MIT1214 strain settled at roughly 30% of total cell numbers as determined by quantitative PCR (Fig. 7E)—providing additional support for our estimate that MIT0917 partially reduces and excretes up to 30% of the NO_3^- transported into the cell as extracellular NO_2^-.

When MIT1214 was paired with MIT0915, a strain that does not produce NO_2^- when growing on NO_3^- in pure culture (Fig. 6A and E), we expected the growth of MIT1214 to stop after any carry-over NO_2^- from the inoculum was exhausted. On the contrary, MIT1214 continued to grow (Fig. 8D) but at significantly lower growth rates compared to either growth in the presence of MIT0917 using NO_3^- as the N source (Fig. 7D) or to the growth of MIT1214 in pure culture using NO_2^- (Fig. 6D). As expected, NO_2^- did not accumulate during the growth of the MIT1214-MIT0915 co-culture (Fig. 8A and B). The frequency of the MIT1214 strain was driven to <5% of total cell numbers over the course of two sequential transfers (Fig. 8E), likely as a consequence of the MIT1214 strain's depressed growth rate in the presence of the MIT0915 strain.

One possible explanation for the MIT1214 strain's continued slow growth in the presence of MIT0915 may be the release of N-containing organic compounds by its partner strain. *Prochlorococcus*, including those belonging to the LLI clade, have been observed to release some N-containing metabolites (33) that could additionally be packaged into vesicles along with DNA or proteins (34). Alternatively, the continued slow growth of MIT1214 suggests the possibility that MIT0915 does produce low quantities of NO_2^- when growing on NO_3^-. Recall that MIT0915 also possesses a FocA NO_2^--specific transporter (Fig. 4)—in contrast to MIT0917—which may facilitate some reuptake of NO_2^- and thus maintain undetectable NO_2^- concentrations in pure culture (Fig. 6A and

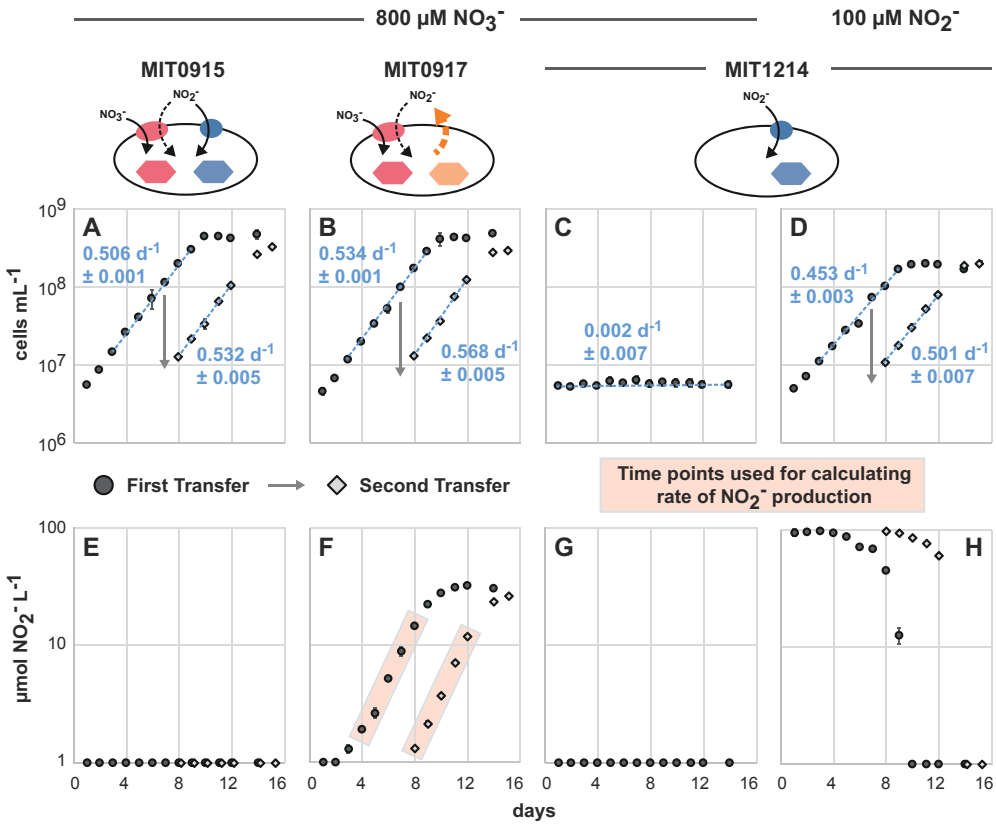

FIG 6 Duplicate pure cultures of MIT0915, MIT0917, and MIT1214 followed over two transfers (transfer 1 in black circles followed by transfer 2 in gray diamonds, with the day of the transfer indicated by the arrow) as contemporaneous controls for co-culture experiments. Mean cell concentrations (A–D) for each transfer are shown with error bars representing standard deviations. Growth rates (mean and standard deviation of μ for each replicate culture) are shown as blue text with the regression shown as a dashed blue line inclusive of the data points used to calculate growth rates. Mean NO_2^- concentrations (E–H) for each transfer are shown with error bars representing standard deviations. NO_2^- concentrations below the dynamic range of the assay (<1 μM NO_2^-) are plotted on the *x*-axis. As pure cultures, MIT0915 and MIT0917 grow using NO_3^- (A, B), but only MIT0917 does so with concomitant release of NO_2^- (E, F). Red shading denotes data points (F) used to calculate cell-specific rates of nitrite release by MIT0917: 4.6×10^{-8} ($\pm 1.5 \times 10^{-8}$) and 5.4×10^{-8} ($\pm 0.54 \times 10^{-8}$) nmol NO_2^- $cell^{-1}$ d^{-1} for the first and second transfers, respectively. MIT1214 cannot use NO_3^- as a N source (C) but has retained the genes necessary for growth on NO_2^- (D, H).

E). Supply of NO_2^- at rates that keep the concentration of NO_2^- at or below MIT1214's half-saturation constant (Ks) for growth on NO_2^- (the concentration of NO_2^- at which the growth rate is half the maximum growth rate) would be consistent with its significantly lower growth rate when co-cultured with MIT0915.

Causes and consequences of incomplete assimilatory NO_3^- reduction by *Prochlorococcus*

Our work has uncovered new potential links between *Prochlorococcus* and the N cycle by demonstrating that some *Prochlorococcus* divert a sizable fraction of transported NO_3^- to extracellular pools of NO_2^- when grown under N-replete batch culture conditions. An intriguing feature of this phenomenon is the degree of phenotypic variability (Fig. 1, 3 and 6F) that maps onto each strain's particular version of the NO_3^- assimilation gene cluster (10). Given the global abundance of *Prochlorococcus* in the world's oceans, this new feature of *Prochlorococcus* could have important consequences for our understanding of primary production and N cycle processes that occur in the tropical and subtropical ocean.

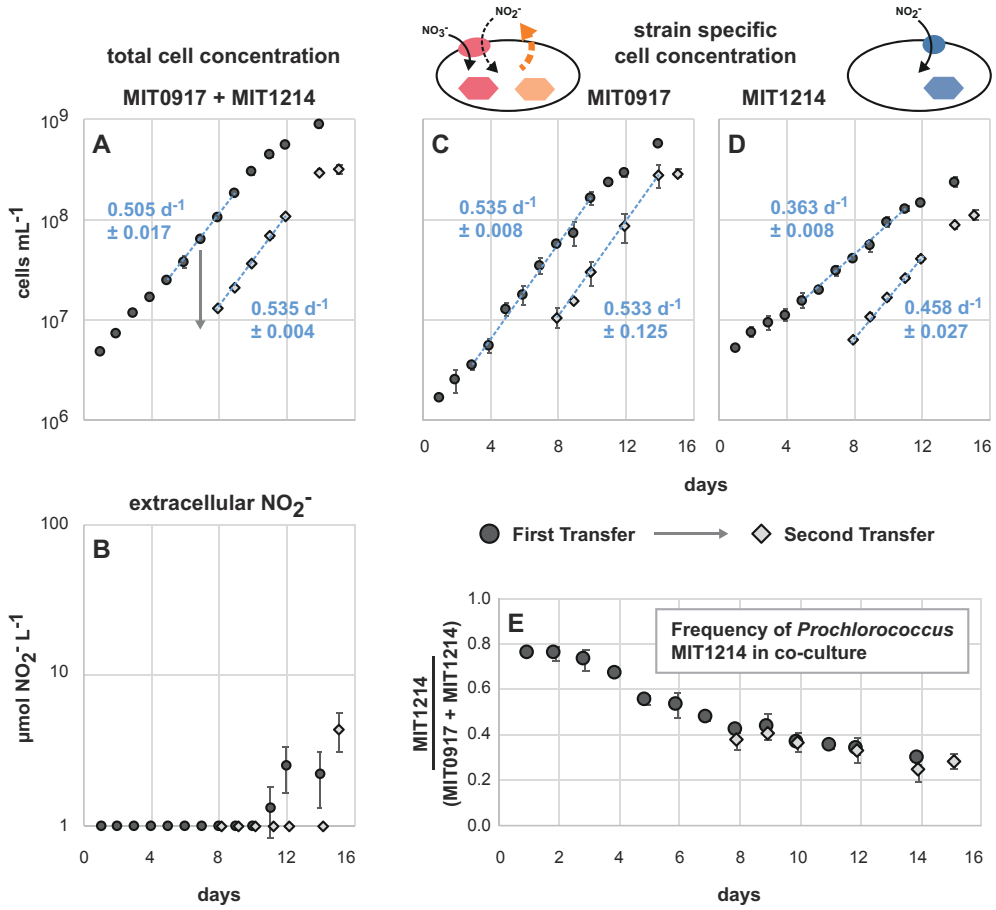

FIG 7 Triplicate co-cultures of *Prochlorococcus* MIT0917 (NO_2^- producer) and *Prochlorococcus* MIT1214 (NO_2^- consumer) over two transfers (transfer 1 in black circles followed by transfer 2 in gray diamonds, with the day of the transfer indicated by the arrow). Each data point represents the mean and standard deviation (error bars) for (A) total cell concentration determined by flow cytometry, (B) NO_2^- concentration, (C, D) strain-specific cell concentration determined by quantitative PCR, and (E) the fraction of MIT1214 cells relative to the sum of cell counts assessed by quantitative PCR. Growth rates (mean and standard deviation of µ for each replicate culture) are shown as blue text with the regression shown as a dashed blue line inclusive of the data points used to calculate growth rates. NO_2^- concentrations below the dynamic range of the assay (<1 µM NO_2^-) are plotted on the *x*-axis.

While many eukaryotic phytoplankton exhibit incomplete assimilatory NO_3^- reduction, this process is not well constrained for the picocyanobacteria that dominate the expansive subtropical gyres of the open ocean. Why would an organism such as *Prochlorococcus*, which is well adapted to life in oligotrophic habitats, release N back into its environment when this nutrient is often in limited supply? Our observations could be related to laboratory culture conditions where the concentrations of inorganic nutrients are much higher than would be observed in the field. Yet, only one functional type of LLI *Prochlorococcus* (represented by the MIT0917 strain) exhibited incomplete assimilatory NO_3^- reduction. It is possible that the divergent version of the NirA NO_2^- reductase possessed by MIT0917—and similar *Prochlorococcus* in the field—has distinct biochemical features. One hypothesis is that this divergent NirA has a higher substrate affinity, perhaps providing these cells with an advantage under chronically N-limited conditions, such as at HOT in the North Pacific Subtropical Gyre (Fig. 5). Under replete conditions in batch culture, these cells might experience a kinetic bottleneck at the NO_2^- reduction step of the NO_3^- assimilation pathway that results in cellular accumulation of NO_2^- because NO_3^- reduction outpaces the k_{cat} of this divergent NirA. This NO_2^- could then diffuse out of the cell as nitrous acid (HNO_2) which would make up a small fraction

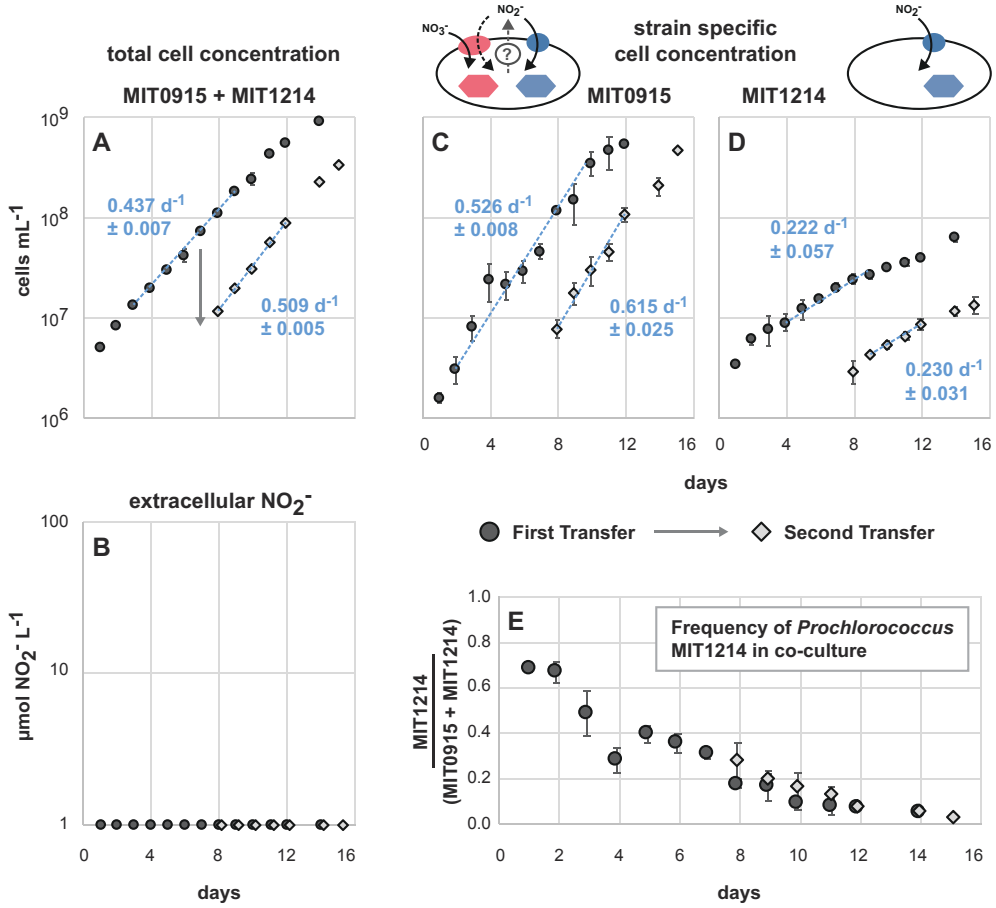

FIG 8 Triplicate co-cultures of *Prochlorococcus* MIT0915 and *Prochlorococcus* MIT1214 over two transfers (transfer 1 in black circles followed by transfer 2 in gray diamonds, with the day of the transfer indicated by the arrow). Each data point represents the mean and standard deviation (error bars) for (A) total cell concentration determined by flow cytometry, (B) NO_2^- concentration, (C, D) strain-specific cell concentration determined by quantitative PCR, and (E) the fraction of MIT1214 cells relative to the sum of cell counts assessed by quantitative PCR. Growth rates (mean and standard deviation of µ for each replicate culture) are shown as blue text with the regression shown as a dashed blue line inclusive of the data points used to calculate growth rates. NO_2^- concentrations below the dynamic range of the assay (<1 µM NO_2^-) are plotted on the *x*-axis.

of the intracellular NO_2^- pool at cellular pH (29). Analogous field conditions would be intermittent upwellings of NO_3^- that temporarily increase local substrate supply (35). We assessed the response of MIT0917 to a similar pulse by washing cells with media that was not amended with NO_3^- in order to remove residual N from the cells. These washed cells were starved of NO_3^- for 3 h and then spiked with either 2 µM NO_3^- or 2 µM NH_4^+ (Supplementary Materials and Methods). At an NO_3^- concentration that was representative of these intermittent pulses of NO_3^- in the wild, MIT0917 released NO_2^- at a cell-specific rate of 6.1×10^{-8} ($\pm 0.28 \times 10^{-8}$) nmol NO_2^- $cell^{-1}$ d^{-1} (Fig. S3).

Prochlorococcus MIT0917 also lacks the FocA NO_2^--specific transporter that is found in other LLI *Prochlorococcus* (Fig. 4), including the MIT0915 strain that does not exhibit extracellular accumulation of NO_2^- in batch culture. An alternative, but not mutually exclusive, hypothesis for NO_2^- release by MIT0917 is that this strain lacks the capacity for cyclic retention of NO_2^- that may diffuse out of the cell as HNO_2. It is common for bacteria to employ so-called "futile cycles" to mitigate the loss of nutrients and metabolites across the cell membrane (36, 37). While this process expends energy, it can serve to regulate substrate retention and maintain sufficiently high concentrations of a substrate within the cell. MIT0917 may not require reuptake of NO_2^- if its NirA is optimized for low internal substrate concentrations—in such a scenario, the *focA* gene

could have been lost due to a general bias toward gene deletion in the absence of a sufficient selective advantage. The MIT0915 strain, on the other hand, might require a mechanism for cyclic retention of NO_2^- if its NirA has a lower substrate affinity.

Our laboratory-based observations suggest that *Prochlorococcus* may interact with the primary NO_2^- maximum layer in complicated ways. In addition to eroding the primary NO_2^- maximum layer through NO_2^- uptake and assimilation, *Prochlorococcus* also appears to have the potential to amplify the magnitude of the primary NO_2^- maximum layer. At present, it is unclear if *Prochlorococcus* exhibit NO_2^- release in the wild and, if so, what abiotic and biotic factors might influence NO_2^- cycling in these populations. Extrapolating from NO_2^- production rates for both *Prochlorococcus* and ammonia-oxidizing archaea as well as the abundance of marker genes for these microbes in the field, we postulate that NO_2^- production by *Prochlorococcus* could be responsible for some degree of NO_2^- produced in the euphotic zone. *Prochlorococcus* MIT0917 releases NO_2^- at rates from 2×10^{-8} nmol NO_2^- cell^{-1} d^{-1} up to 7×10^{-8} nmol NO_2^- cell^{-1} d^{-1} (Fig. 3). In comparison, the dominant ammonia-oxidizing microorganism in subtropical open ocean ecosystems, *Candidatus* Nitrosopelagicus brevis (38), produces NO_2^- at a rate of about 2×10^{-6} nmol NO_2^- cell^{-1} d^{-1} in batch culture (39). Ammonia-oxidizing archaea are thus expected to produce NO_2^- at 30- to 100-fold higher rates than *Prochlorococcus*, but the latter is often more abundant. For instance, ammonia-oxidizing archaea in the epipelagic zone have been typically observed at abundances of 1,000–6,000 *amoA* gene copies mL^{-1} (16, 40, 41). Low-light-adapted *Prochlorococcus* with the capacity of NO_3^- assimilation, however, can reach abundances of 1,000–40,000 cells mL^{-1} in the vicinity of the subsurface chlorophyll maximum layer (9). Therefore, depending on both rates and cell abundances, *Prochlorococcus* could be responsible from anywhere between <1% to approximately 50% of NO_2^- production in the mid-euphotic zone as a fraction of *Prochlorococcus* and nitrifier-derived NO_2^-.

As we have demonstrated, different functional types of *Prochlorococcus* can coexist under conditions where NO_2^- cross-feeding is promoted and NO_2^- accumulation is minimized (Fig. 7). Consequently, NO_2^- production and consumption in *Prochlorococcus* populations might be a cryptic process whereby there is no net accumulation of NO_2^- at steady state. In the wild, *Prochlorococcus* populations could dynamically assemble in response to the availability of N sources of varying redox state as well as in response to community-wide competition for these N sources. Net NO_2^- accumulation might only occur within these populations during periods of perturbation (e.g., changes in light intensity or nutrient supply). Additional study is warranted to examine the conditions under which *Prochlorococcus* populations are either net producers or net consumers of NO_2^- and evaluate how microbial populations and communities modulate the availability of various N sources that ultimately impact production and remineralization processes. At the population level, the dynamic assembly of distinct functional types of *Prochlorococcus* could emerge through interactions that are mediated, in part, by cross-feeding of NO_2^-. We posit that trait variability and the selection of complementary functions might facilitate robustness or resiliency in microbial populations. *Prochlorococcus*, as a key primary producer in the tropical and subtropical oceans, offers an extremely valuable lens through which to constrain the rules under which emergent features arise.

MATERIALS AND METHODS

Strains

The cultures used in this study included the low-light-adapted *Prochlorococcus* strains MIT0915 (LLI clade), MIT0917 (LLI clade), and MIT1214 (LLI clade), the high-light-adapted *Prochlorococcus* strain SB (HLII clade), as well as *Synechococcus* strains WH8102 (clade III) and WH7803 (clade V) (Table S1).

NO_2^- production rates

The NO_3^- assimilating strains (MIT0915, MIT0917, SB, WH7803, and WH8102) were grown in triplicate as pure cultures using Pro99 medium (natural seawater base; Sargasso Seawater) with the 800 µM ammonium chloride (NH_4Cl) omitted and replaced by 800 µM sodium nitrate ($NaNO_3$). The cultures were grown in 35 mL of medium in borosilicate glass culture tubes at a temperature of 24°C and under continuous illumination intensities of 6, 36, 52, and 85 µmol photons m^{-2} s^{-1}. Given that the strains represent multiple clades of *Prochlorococcus* and *Synechococcus* that span a wide range of depths and light wavelengths in the euphotic zone, we used white light provided by fluorescent lamps. The LLI strains (MIT0915 and MIT0917) had poor and inconsistent growth at the highest light intensity, so these strains were only examined at the three lower light intensities (6, 36, and 52 µmol photons m^{-2} s^{-1}). Cultures were monitored daily by removing 0.5 mL of culture in order to determine cell abundances with flow cytometry and NO_2^- concentrations with the Griess colorimetric method (Supplementary Materials and Methods). Net cell-specific NO_2^- production rates were calculated as the change in NO_2^- concentration relative to the logarithmic mean of cell concentrations—to account for exponential growth—for successive time points during the log-linear portion of the growth curve.

Co-culture experiments

MIT1214 was co-cultured, in triplicate, with either MIT0915 or MIT0917 in 35 mL of medium in borosilicate glass culture tubes using NO_3^- as the sole N source at 24°C. In order to approximate the light intensities and wavelengths that LLI *Prochlorococcus* typically experience in the wild (12, 42, 43), while still maintaining high growth rates, the cultures were grown at 16 µmol photons m^{-2} s^{-1} of continuous blue light (in lieu of white light). As controls, all strains were grown as pure cultures, in duplicate, under the same temperature and light conditions. The MIT1214-MIT0915 and MIT1214-MIT0917 co-cultures, as well as the MIT0915 and MIT0917 pure cultures, used Pro99 medium (natural seawater base; Sargasso Seawater) with 800 µM sodium nitrate ($NaNO_3$) as the sole N source. Pure cultures of MIT1214 were grown in Pro99 medium using 100 µM sodium nitrite ($NaNO_2$) as the sole N source to serve as a control for growth on NO_2^-. Given that some strains of *Prochlorococcus* might be inhibited by NO_2^- (44), a lower concentration of $NaNO_2$ was used (instead of 800 µM) to minimize potential growth inhibition due to NO_2^- toxicity. MIT1214 was also grown in Pro99 medium using 800 µM NO_3^- as the sole N source to serve as control for the absence of growth on NO_3^-. The co-cultures and pure cultures were sampled daily over two sequential transfers to monitor cell abundances with flow cytometry, NO_2^- concentrations using the Griess method, and to preserve cells on filters for strain-specific cell abundance measurements (Supplementary Materials and Methods). Given that the cell size and fluorescence properties of MIT0915, MIT0917, and MIT1214 overlap when examined using flow cytometry (all are LLI clade cells with similar size and chlorophyll content), we used quantitative PCR to assess the cell abundance of each strain in co-culture. Sample processing, standards, reaction conditions, and amplification efficiencies for the qPCR assays are detailed in the Supplementary Materials and Methods.

ACKNOWLEDGMENTS

This work was supported by grants from the National Science Foundation (OCE-2048470 to P.M.B.) and the Simons Foundation (Life Sciences Project Award ID 337262, S.W.C.; SCOPE Award ID 329108, S.W.C.).

The authors thank Rogier Braakman (MIT) for insightful discussions.

AUTHOR AFFILIATIONS

[1]Department of Civil and Environmental Engineering, Massachusetts Institute of Technology, Cambridge, Massachusetts, USA
[2]Department of Biology, Massachusetts Institute of Technology, Cambridge, Massachusetts, USA

PRESENT ADDRESS

Tyler J. O'Keefe, Department of Earth, Marine, and Environmental Sciences, University of North Carolina at Chapel Hill, Chapel Hill, North Carolina, USA
Anna Rasmussen, Department of Earth System Science, Stanford University, Palo Alto, California, USA

AUTHOR ORCIDs

Paul M. Berube http://orcid.org/0000-0001-5598-6602

FUNDING

Funder	Grant(s)	Author(s)
National Science Foundation (NSF)	OCE-2048470	Paul M. Berube
Simons Foundation (SF)	337262, 329108	Sallie W. Chisholm

AUTHOR CONTRIBUTIONS

Paul M. Berube, Conceptualization, Data curation, Formal analysis, Funding acquisition, Investigation, Methodology, Project administration, Supervision, Validation, Visualization, Writing – original draft, Writing – review and editing | Tyler J. O'Keefe, Data curation, Investigation, Methodology, Validation, Writing – review and editing | Anna Rasmussen, Data curation, Investigation, Methodology, Validation, Writing – review and editing | Trent LeMaster, Investigation, Methodology, Validation | Sallie W. Chisholm, Funding acquisition, Resources, Supervision, Writing – review and editing

DIRECT CONTRIBUTION

This paper is a contribution from the Simons Collaboration on Ocean Processes and Ecology (SCOPE).

DATA AVAILABILITY

Genome assemblies are available from NCBI GenBank under the following accession numbers: CP114781 (*Prochlorococcus* MIT0915), CP114784 (*Prochlorococcus* MIT0917), CP114777 (*Prochlorococcus* MIT1214), JNAS00000000 (*Prochlorococcus* SB), CT971583 (*Synechococcus* WH7803), BX548020 (*Synechococcus* WH8102). Genome annotations are available from the DOE Joint Genome Institute's Integrated Microbial Genomes and Microbiomes System (IMG/M) under the following accession numbers: 2681812901 (*Prochlorococcus* MIT0915), 2681812859 (*Prochlorococcus* MIT0917), 2681813567 (*Prochlorococcus* MIT1214), 2606217677 (*Prochlorococcus* SB), 640427149 (*Synechococcus* WH7803) and 637000314 (*Synechococcus* WH8102). Cell density and NO_2^- concentration data are available under dataset 890887 from the Biological and Chemical Oceanography Data Management Office (BCO-DMO).

ADDITIONAL FILES

The following material is available online.

Supplemental Material

Supplemental material (supplemental.mBio.01236-23-s0001.pdf). Supplemental Materials and Methods, Tables S1 and S2, and Figures S1 to S3.

REFERENCES

1. Flombaum P, Gallegos JL, Gordillo RA, Rincón J, Zabala LL, Jiao N, Karl DM, Li WKW, Lomas MW, Veneziano D, Vera CS, Vrugt JA, Martiny AC. 2013. Present and future global distributions of the marine cyanobacteria *Prochlorococcus* and *Synechococcus*. Proc Natl Acad Sci U S A 110:9824–9829. https://doi.org/10.1073/pnas.1307701110
2. Tyrrell T. 1999. The relative influences of nitrogen and phosphorus on oceanic primary production. Nature 400:525–531. https://doi.org/10.1038/22941
3. Ohashi Y, Shi W, Takatani N, Aichi M, Maeda S, Watanabe S, Yoshikawa H, Omata T. 2011. Regulation of nitrate assimilation in cyanobacteria. J Exp Bot 62:1411–1424. https://doi.org/10.1093/jxb/erq427
4. Coleman ML, Chisholm SW. 2007. Code and context: *Prochlorococcus* as a model for cross-scale biology. Trends Microbiol 15:398–407. https://doi.org/10.1016/j.tim.2007.07.001
5. Kettler GC, Martiny AC, Huang K, Zucker J, Coleman ML, Rodrigue S, Chen F, Lapidus A, Ferriera S, Johnson J, Steglich C, Church GM, Richardson P, Chisholm SW. 2007. Patterns and implications of gene gain and loss in the evolution of *Prochlorococcus*. PLoS Genet 3:e231. https://doi.org/10.1371/journal.pgen.0030231
6. Biller SJ, Berube PM, Lindell D, Chisholm SW. 2015. *Prochlorococcus*: the structure and function of collective diversity. Nat Rev Microbiol 13:13–27. https://doi.org/10.1038/nrmicro3378
7. Martiny AC, Kathuria S, Berube PM. 2009. Widespread metabolic potential for nitrite and nitrate assimilation among *Prochlorococcus* ecotypes. Proc Natl Acad Sci U S A 106:10787–10792. https://doi.org/10.1073/pnas.0902532106
8. Berube PM, Biller SJ, Kent AG, Berta-Thompson JW, Roggensack SE, Roache-Johnson KH, Ackerman M, Moore LR, Meisel JD, Sher D, Thompson LR, Campbell L, Martiny AC, Chisholm SW. 2015. Physiology and evolution of nitrate acquisition in *Prochlorococcus*. ISME J 9:1195–1207. https://doi.org/10.1038/ismej.2014.211
9. Berube PM, Coe A, Roggensack SE, Chisholm SW. 2016. Temporal dynamics of *Prochlorococcus* cells with the potential for nitrate assimilation in the subtropical Atlantic and Pacific oceans. Limnol Oceanogr 61:482–495. https://doi.org/10.1002/lno.10226
10. Berube PM, Rasmussen A, Braakman R, Stepanauskas R, Chisholm SW. 2019. Emergence of trait variability through the lens of nitrogen assimilation in *Prochlorococcus*. Elife 8:e41043. https://doi.org/10.7554/eLife.41043
11. Johnson ZI, Zinser ER, Coe A, McNulty NP, Woodward EMS, Chisholm SW. 2006. Niche partitioning among *Prochlorococcus* ecotypes along ocean-scale environmental gradients. Science 311:1737–1740. https://doi.org/10.1126/science.1118052
12. Malmstrom RR, Coe A, Kettler GC, Martiny AC, Frias-Lopez J, Zinser ER, Chisholm SW. 2010. Temporal dynamics of *Prochlorococcus* ecotypes in the Atlantic and Pacific oceans. ISME J 4:1252–1264. https://doi.org/10.1038/ismej.2010.60
13. Brandhorst W. 1959. Nitrification and denitrification in the eastern tropical North Pacific. ICES J Marine Sci 25:3–20. https://doi.org/10.1093/icesjms/25.1.3
14. Lomas MW, Lipschultz F. 2006. Forming the primary nitrite maximum: nitrifiers or phytoplankton?. Limnol Oceanogr 51:2453–2467. https://doi.org/10.4319/lo.2006.51.5.2453
15. Olson RJ. 1981. Differential Photoinhibition of Marine Nitrifying bacteria: A possible mechanism for the formation of the primary nitrite maximum. J Mar Res 39:227–238. https://elischolar.library.yale.edu/journal_of_marine_research/1541.
16. Zakem EJ, Al-Haj A, Church MJ, van Dijken GL, Dutkiewicz S, Foster SQ, Fulweiler RW, Mills MM, Follows MJ. 2018. Ecological control of nitrite in the upper ocean. Nat Commun 9:1206. https://doi.org/10.1038/s41467-018-03553-w
17. Vaccaro RF, Ryther JH. 1960. Marine phytoplankton and the distribution of nitrite in the sea. ICES Journal of Marine Science 25:260–271. https://doi.org/10.1093/icesjms/25.3.260
18. Collos Y. 1998. Nitrate uptake, nitrite release and uptake, and new production estimates. Mar Ecol Prog Ser 171:293–301. https://doi.org/10.3354/meps171293
19. Laws EA, Wong DCL. 1978. Studies of carbon and nitrogen metabolism by three marine phytoplankton species in nitrate-limited continuous culture. J Phycol 14:406–416. https://doi.org/10.1111/j.1529-8817.1978.tb02460.x
20. Sciandra A, Amara R. 1994. Effects of nitrogen limitation on growth and nitrite excretion rates of the dinoflagellate. Mar Ecol Prog Ser 105:301–309. https://doi.org/10.3354/meps105301
21. Raimbault P. 1986. Effect of temperature on nitrite excretion by three marine diatoms during nitrate uptake. Marine Biology 92:149–155. https://doi.org/10.1007/BF00392831
22. Serra JL, Llama MJ, Cadenas E. 1978. Nitrate utilization by the diatom *Skeletonema costatum*: I. Kinetics of nitrate uptake. Plant Physiol 62:987–990. https://doi.org/10.1104/pp.62.6.987
23. Olson RJ, Soohoo JB, Kiefer DA. 1980. Steady-state growth of the marine diatom *Thalassiosira pseudonana*: uncoupled kinetics of nitrate uptake and nitrite production. Plant Physiol 66:383–389. https://doi.org/10.1104/pp.66.3.383
24. Colios Y. 1982. Transient situations in nitrate assimilation by marine diatoms. 2. Changes in nitrate and nitrite following a nitrate perturbation. Limnol Oceanogr 27:528–535. https://doi.org/10.4319/lo.1982.27.3.0528
25. Milligan AJ, Harrison PJ. 2000. Effects of non-steady-state iron limitation on nitrogen assimilatory enzymes in the marine diatom *Thalassiosira weissflogii* (Bacillariophyceae). J Phycol 36:78–86. https://doi.org/10.1046/j.1529-8817.2000.99013.x
26. Martinez R. 1991. Transient nitrate uptake and assimilation in *Skeletonema costatum* cultures subject to nitrate starvation under low irradiance. J Plankton Res 13:499–512. https://doi.org/10.1093/plankt/13.3.499
27. Cordero OX, Polz MF. 2014. Explaining microbial genomic diversity in light of evolutionary ecology. Nat Rev Microbiol 12:263–273. https://doi.org/10.1038/nrmicro3218
28. Aichi M, Yoshihara S, Yamashita M, Maeda S, Nagai K, Omata T. 2006. Characterization of the nitrate-nitrite transporter of the major facilitator superfamily (the nrtP gene product) from the cyanobacterium Nostoc punctiforme strain ATCC 29133. Biosci Biotechnol Biochem 70:2682–2689. https://doi.org/10.1271/bbb.60286
29. Kiefer DA, Olson RJ, Holm-Hansen O. 1976. Another look at the nitrite and chlorophyll maxima in the central North Pacific. Deep Sea Res Oceanogr Abstr 23:1199–1208. https://doi.org/10.1016/0011-7471(76)90895-0
30. Berges JA, Varela DE, Harrison PJ. 2002. Effects of temperature on growth rate, cell composition and nitrogen metabolism in the marine diatom *Thalassiosira pseudonana* (Bacillariophyceae). Mar Ecol Prog Ser 225:139–146. https://doi.org/10.3354/meps225139
31. Heldal M, Scanlan DJ, Norland S, Thingstad F, Mann NH. 2003. Elemental composition of single cells of various strains of marine *Prochlorococcus* and *Synechococcus* using X-ray microanalysis. Limnol Oceanogr 48:1732–1743. https://doi.org/10.4319/lo.2003.48.5.1732
32. Biller SJ, Berube PM, Dooley K, Williams M, Satinsky BM, Hackl T, Hogle SL, Coe A, Bergauer K, Bouman HA, Browning TJ, De Corte D, Hassler C, Hulston D, Jacquot JE, Maas EW, Reinthaler T, Sintes E, Yokokawa T, Chisholm SW. 2018. Marine microbial metagenomes sampled across space and time. Sci Data 5:180176. https://doi.org/10.1038/sdata.2018.176
33. Kujawinski EB, Braakman R, Longnecker K, Chisholm SW, Becker JW, Dooley K, Soule MCK, Swarr GJ, Halloran K. 2022. Metabolite diversity among *Prochlorococcus* strains belonging to divergent ecotypes. bioRxiv. https://doi.org/10.1101/2022.12.20.521339
34. Biller SJ, Lundeen RA, Hmelo LR, Becker KW, Arellano AA, Dooley K, Heal KR, Carlson LT, Van Mooy BAS, Ingalls AE, Chisholm SW. 2022.

Prochlorococcus extracellular vesicles: molecular composition and adsorption to diverse microbes. Environ Microbiol 24:420–435. https://doi.org/10.1111/1462-2920.15834
35. Johnson KS, Riser SC, Karl DM. 2010. Nitrate supply from deep to near-surface waters of the North Pacific subtropical gyre. Nature 465:1062–1065. https://doi.org/10.1038/nature09170
36. Ritchie RJ. 2013. The ammonia transport, retention and futile cycling problem in cyanobacteria. Microb Ecol 65:180–196. https://doi.org/10.1007/s00248-012-0111-1
37. Neijssel OM, Buurman ET, Teixeira de Mattos MJ. 1990. The role of futile cycles in the energetics of bacterial growth. Biochim Biophys Acta 1018:252–255. https://doi.org/10.1016/0005-2728(90)90260-b
38. Santoro AE, Dupont CL, Richter RA, Craig MT, Carini P, McIlvin MR, Yang Y, Orsi WD, Moran DM, Saito MA. 2015. Genomic and proteomic characterization of "*Candidatus Nitrosopelagicus brevis*": an ammonia-oxidizing archaeon from the open ocean. Proc Natl Acad Sci U S A 112:1173–1178. https://doi.org/10.1073/pnas.1416223112
39. Santoro AE, Casciotti KL. 2011. Enrichment and characterization of ammonia-oxidizing archaea from the open ocean: phylogeny, physiology and stable isotope fractionation. ISME J 5:1796–1808. https://doi.org/10.1038/ismej.2011.58
40. Santoro AE, Saito MA, Goepfert TJ, Lamborg CH, Dupont CL, DiTullio GR. 2017. Thaumarchaeal ecotype distributions across the equatorial Pacific ocean and their potential roles in nitrification and sinking flux attenuation. Limnol Oceanogr 62:1984–2003. https://doi.org/10.1002/lno.10547
41. Sintes E, De Corte D, Haberleitner E, Herndl GJ. 2016. Geographic distribution of archaeal ammonia oxidizing ecotypes in the Atlantic ocean. Front Microbiol 7:77. https://doi.org/10.3389/fmicb.2016.00077
42. Letelier RM, Karl DM, Abbott MR, Bidigare RR. 2004. Light driven seasonal patterns of chlorophyll and nitrate in the lower euphotic zone of the North Pacific Subtropical Gyre. Limnol Oceanogr 49:508–519. https://doi.org/10.4319/lo.2004.49.2.0508
43. Stomp M, Huisman J, Stal LJ, Matthijs HCP. 2007. Colorful niches of phototrophic microorganisms shaped by vibrations of the water molecule. ISME J 1:271–282. https://doi.org/10.1038/ismej.2007.59
44. Moore LR, Post AF, Rocap G, Chisholm SW. 2002. Utilization of different nitrogen sources by the marine cyanobacteria *Prochlorococcus* and *Synechococcus*. Limnol Oceanogr 47:989–996. https://doi.org/10.4319/lo.2002.47.4.0989

Supplemental Material

Production and cross-feeding of nitrite within *Prochlorococcus* populations

Paul M. Berube,[a]# Tyler O'Keefe,[a]* Anna Rasmussen,[a]* Trent LeMaster,[a] Sallie W. Chisholm[a,b]

[a]Department of Civil and Environmental Engineering, Massachusetts Institute of Technology, Cambridge, Massachusetts, USA

[b]Department of Biology, Massachusetts Institute of Technology, Cambridge, Massachusetts, USA

#Correspondence to Paul M. Berube, pmberube@mit.edu.

*Present address: Tyler O'Keefe, Department of Earth, Marine, and Environmental Sciences, University of North Carolina at Chapel Hill, Chapel Hill, North Carolina, USA

*Present address: Anna Rasmussen, Department of Earth System Science, Stanford University, Palo Alto, California, USA

This PDF file includes:

- Supplementary Materials and Methods
- Table S1 – *Prochlorococcus* and *Synechococcus* strains
- Table S2 – NCBI and IMG accession numbers and the genetic inventory of nitrate and nitrite assimilation genes for the *Prochlorococcus* and *Synechococcus* strains
- Fig. S1 – Extracellular NO_2^- during the growth of *Prochlorococcus* on NH_4^+
- Fig. S2 – Extracellular NO_2^- during the growth of *Synechococcus* on NH_4^+
- Fig. S3 – NO_2^- release by *Prochlorococcus* MIT0917 at low NO_3^- concentrations
- Supplementary References

SUPPLEMENTARY MATERIALS AND METHODS

Strains. The cultures used in this study are detailed in Table S1. *Prochlorococcus* MIT1214 was isolated from an enrichment culture initiated as part of the Hawaii Ocean Experiment-Dynamics of Light and Nutrients (HOE-DYLAN) VII expedition (UNOLS Cruise ID: KM1217) at coordinates 22.8^{o}N and -158.0^{o}E. Unfiltered seawater from 175m was aliquoted into acid-washed 30 mL polycarbonate oakridge tubes and amended with 16 µM sodium nitrate, 1 µM sodium phosphate, 0.117 µM ethylenediaminetetraacetic acid, 0.117 µM iron(III) chloride, 0.0090 µM manganese(II) chloride, 0.0008 µM zinc(II) sulfate, 0.0005 µM cobalt(II) chloride, 0.0003 µM sodium molybdate, 0.0010 µM sodium selenite, and 0.0010 µM nickel(II) chloride. Enrichment cultures were routinely monitored by flow cytometry and those exhibiting growth of a *Prochlorococcus*-like population were transferred into fresh medium and ultimately acclimated to growth on Pro99 medium. As part of our study, MIT1214, MIT0915, and MIT0917 were rendered axenic by dilution to extinction (1). All strains were routinely assayed for heterotrophic contaminants by staining cells with SYBR green and assessing the fluorescence and light scattering properties of both stained and unstained cells using a Guava easyCyte 12HT Flow Cytometer (MilliporeSigma, Burlington, MA, USA) – cultures that did not exhibit the presence of non-photosynthetic cells in the stained samples and had a single cyanobacteria population were presumed axenic and unialgal. All axenic cultures were routinely assessed for purity by confirming a lack of turbidity after inoculation into a panel of purity test broths as described previously (1).

Genome sequencing. The genome of MIT1214 was sequenced as follows. Cells were grown to mid exponential phase and pelleted by centrifugation. DNA was isolated by phenol/chloroform extraction (2). PacBio library preparation and sequencing was carried out by

the MIT BioMicro Center and the UMass Worcester Medical School's Deep Sequencing Core Facility. Assembly of PacBio reads was performed using the hierarchical genome-assembly process (Protocol = RS_HGAP_Assembly.2) as implemented in SMRT Analysis 2.3.0 (3) with the following parameters adjusted: Minimum Polymerase Read Quality = 0.85 and Genome Size = 2000000 bp (default settings were used for all other parameters). Overlapping ends of the assembly were identified using BLAST and the assembly was manually circularized. Circular assemblies were corrected using the RS_Resequencing.1 protocol in SMRT Analysis 2.3.0 (3) with the following parameters: Minimum Polymerase Read Quality = 0.85 and Consensus Algorithm = Quiver. The MIT1214 genome was annotated using IMG Annotation Pipeline version 4 (4, 5), and included in ProPortal CyCOGs 6.0 (6).

Rationale for strain selection. Strains were selected to encompass the observed variations in the NO_3^- and NO_2^- assimilation gene cluster for *Prochlorococcus* and *Synechococcus*. Among strains belonging to the low-light adapted LLI clade of *Prochlorococcus*, we have identified 3 configurations of the NO_3^- and NO_2^- assimilation gene cassette (7), each represented in our study by the MIT1214, MIT0915, and MIT0917 strains (Tables S1 and S2). MIT1214 has the capacity for NO_2^- assimilation, but not NO_3^- assimilation – i.e., it has lost the upstream half of the NO_3^- assimilation pathway, but has retained the downstream half for the assimilation of the more reduced NO_2^-. MIT0915 can assimilate NO_3^- and also possesses a NO_2^- specific transporter (FocA) and a NO_2^- reductase (NirA) that are both closely related to those found in MIT1214. MIT0917 can also assimilate NO_3^-, but in contrast to MIT0915, this strain has a divergent version of NirA and has also lost the gene encoding the FocA NO_2^- transporter (7). We also examined a representative of the high-light adapted HLII clade of *Prochlorococcus*, strain SB (Table S1). SB possesses the full pathway for NO_3^- and

NO_2^- assimilation, except for the FocA NO_2^- transporter (7). The *Synechococcus* strains examined included WH7803 and WH8102, the latter of which is adapted to warm oligotrophic waters and has a range that overlaps with the abundant HLII clade of *Prochlorococcus* (8). Both of these *Synechococcus* strains possess the full pathway for NO_3^- and NO_2^- assimilation, with WH7803 having retained the FocA NO_2^- transporter and WH8102 having lost it.

NO_2^- determination. Extracellular NO_2^- concentrations were determined via the Greiss colorimetric method that reacts sulfanilamide and *N*-(1-naphthyl)ethylenediamine (NED) with NO_2^- to produce a pink-red azo dye with a maximum absorption at a wavelength of 540 nm. A color reagent solution of 1% (10 mg mL^{-1}) sulfanilamide, 5% 12M HCl, and 0.1% (1 mg mL^{-1}) NED was filtered through a 0.2um filter into UV resistant bottles. Aliquots of a 1 mM sodium nitrite ($NaNO_2$) standard solution was stored frozen at -20°C and thawed daily to prepare dilutions spanning 1-50 µM for the generation of a standard curve. To prepare samples for quantification of NO_2^- , 0.15 mL was removed from cultures and filtered through a 96-well 0.45µm MultiScreenHTS HVfilter plate (MilliporeSigma, Burlington, MA, USA) capable of capturing >99% of *Prochlorococcus* cells. Dilutions of the $NaNO_2$ standard were filtered in the same plate as the culture samples to ensure similar treatment. 100uL of filtrate was then transferred from each well to a flat-bottomed, 96-well microplate. An equal volume of color reagent (100 uL) was added to each well, mixed by pipetting, and incubated in the dark for 20 minutes to allow for color development. Absorbance at 540 nm was then determined by using a Synergy 2 Plate Reader (BioTek Instruments, Winooski, VT, USA).

Setup and sampling of co-cultures. Pure cultures of MIT0915, MIT0917, and MIT1214 were passaged twice at 24°C and 16 µmol photons m^{-2} s^{-1} of blue light in Pro99 medium using 800 µM NO_3^- as the sole N source for MIT0915 and MIT0917 and 100 µM NO_2^- as the sole N

source for MIT1214. Cell concentrations were then determined using flow cytometry on a Guava easyCyte 12HT Flow Cytometer (MilliporeSigma, Burlington, MA, USA). Co-cultures were established by inoculating fresh medium with 2 x 10^6 cells mL^{-1} of each strain for a total initial cell concentration of 4 x 10^6 cells mL^{-1}. Pure cultures were inoculated into fresh medium at 4 x 10^6 cells mL^{-1}. Cultures were monitored daily by removing 0.5 mL of culture for flow cytometry and NO_2^- concentration determination as detailed above. Daily samples for quantitative PCR were preserved by filtering 1 mL of culture onto a 25 mm 0.2 µm pore size polycarbonate filter under low vacuum, chasing with 2 mL of qPCR preservation solution (10 mM Tris pH=8, 100 mM EDTA, and 500 mM NaCl), and then transferring the filter to a 2 mL beadbeater tube prior to storage at -80°C. After the initial culture had grown for 7 days, a subsample was transferred into fresh medium at a final cell concentration of 8 x 10^7 cells mL^{-1} (total cells). The initial transfer was monitored for 14 days and the second transfer was monitored for 8 days (i.e., until the cultures began to enter stationary phase as indicated by the daily change in cell concentrations).

Quantitative PCR methods. For MIT0915 and MIT0917, we used an assay that we had previously developed for detection of *narB* in these strains (9). For the detection of MIT1214 we designed a qPCR assay to target the *wckA* gene (encoding a polysaccharide pyruvyl transferase family protein) in MIT1214 that is absent in both MIT0915 and MIT0917. Primers targeting the *wcaK* gene of *Prochlorococcus* MIT1214 were designed using the NCBI Primer-BLAST tool:

Forward Primer, MIT1214_wcaK_283F (5'- GACTACTGCATTTTCGCTGGG - 3')

Reverse Primer, MIT1214_wcaK_402R (5'- ACCTTCAAAACCTCCAACACC - 3')

Samples used to generate standard curves were acquired by growing MIT0915, MIT0917, and MIT1214 to late-exponential phase (approximately 8 x 10^7 cells mL^{-1}), filtering 5 mL of culture

onto a 25 mm 0.2 µm pore size polycarbonate filter under low vacuum, chasing with 3 mL of qPCR preservation solution (10 mM Tris pH=8, 100 mM EDTA, and 500 mM NaCl), and then transferring the filter to a 2 mL beadbeater tube prior to storage at -80°C. Cell concentrations for each culture, at the time of sample filtration, was obtained through flow cytometry. Templates for both experimental cultures and standards were generated by thawing the filters on ice for 2 min, adding 650 µl of 10 mM Tris pH=8, and then beadbeating at 4800 rpm for 2 minutes. Following beadbeating to remove cells from the filter, 500 µl of the buffer was transferred to a 1.5 mL centrifuge tube and heated at 95°C for 15 min to lyse cells. Templates for standard curves were generated by first diluting the resulting template solution to 5.4×10^5 cells μl^{-1} and then performing a serial dilution. All templates were stored at -80°C until use.

The MIT1214 *wcaK* assay was performed in 25 µl reaction volumes with 2.5 µl template and the following final concentrations of reaction components: 12.5 µl QuantiTect SYBR Green PCR Mix (Qiagen, Germantown, Maryland) and 0.5 µmol L^{-1} of each forward and reverse primer. Using a CFX96 Thermocycler (Bio-Rad, Hercules, CA, USA), reactions were pre-incubated at 95°C for 15 min to activate the polymerase and then cycled (40 cycles) at 95°C for 15 s, 57°C for 30 s, and 72°C for 30 s. The MIT0915 and MIT0917 *narB* assays were performed similarly, except for annealing at 60°C for 30 s (9). Amplification efficiencies were 85% for the MIT1214 *wcaK* assay, 90% for the MIT0915 *narB* assay, and 79% for the MIT0917 *narB* assay. Negative controls included MIT0915 and MIT0917 templates for the MIT1214 *wcaK* assay as well as MIT1214 templates for the *narB* assay; no amplification was observed in these negative controls.

Metagenomic derived frequencies of LLI functional types. Paired-end sequencing reads for samples obtained from the subsurface chlorophyll maximum layer at HOT and BATS

(10) were annotated using kaiju 1.7.2 (11) and the MARMICRODB reference database of marine microorganisms (12, 13):

```
kaiju -z 20 \
      -t $DATABASE/nodes.dmp \
      -f $DATABASE/MARMICRODB.fmi \
      -i $READDATADIR/$LIBRARY_1_trimmed.fq \
      -j $READDATADIR/$LIBRARY_2_trimmed.fq \
      -o $LIBRARY_marmicrodb_pairs_kaiju.out -v
```

Reads matching the taxonomic identifier for the LLI clade of *Prochlorococcus* were extracted from the paired-end sequencing reads using seqtk 1.3 (https://github.com/lh3/seqtk). Frequencies of LLI *Prochlorococcus* N assimilation genotypes were determined by further annotation of the taxonomically binned reads using kaiju and the CyCOG v6 database (6). Reads that mapped to the *gyrB, narB*, *focA*, type I *nirA*, and type II *nirA* genes were enumerated and normalized to gene length. We assume that each of these genes are found in single copies in *Prochlorococcus* genomes based on their prevalence in the CyCOG v6 database (6). Fractions of LLI *Prochlorococcus* that belonged to each of the 3 functional types (Fig. 4 in the main text) were resolved using the gene length normalized counts of N assimilation marker genes in each metagenome. Specifically, the abundance of MIT1214-like genomes was operationally defined as length-normalized counts of type I *nirA* genes less the length-normalized counts of *narB* genes. MIT0917-like genomes were defined as the length-normalized counts of type II *nirA* genes. MIT0915-like genomes were defined as the length-normalized counts of *narB* genes less the length-normalized counts of type II *nirA* genes. Each of these values was divided by the length-normalized counts of the *gyrB* gene, a single copy core gene in LLI *Prochlorococcus*, in order to obtain the fraction of the LLI *Prochlorococcus* population represented by each functional type. Seasonality of the frequency of each functional type in LLI *Prochlorococcus*

populations was assessed by binning these data into 4 subsets based on sample collection month – winter (January through March), spring (April through June), summer (July through September), and autumn (October through December).

NO_2^- production at low NO_3^- concentrations. The cell-specific NO_2^- production rate of *Prochlorococcus* MIT0917 was further assessed in cultures amended with 2 μM NO_3^- to explore the potential occurrence of incomplete assimilatory NO_3^- reduction at environmentally relevant NO_3^- concentrations. Growth medium was prepared by using autoclaved seawater obtained from surface waters of the N-limited South Pacific Subtropical Gyre during the MV1015 cruise. Inorganic N in the surface mixed layer at the time of seawater collection was undetectable (14). The sterile seawater was amended with 160 μM sodium nitrate, 10 μM sodium phosphate, and 0.2x of Pro99 trace metals (15). *Prochlorococcus* MIT0917 was grow in duplicate in 250 mL of this medium in 500 mL polyethylene bottles until the cells reached late exponential phase. The cultures were then pelleted at 10,000 RPM in a JA-14 rotor for 15 minutes at 22°C. The spent medium was decanted, leaving approximately 2 mL of residual liquid. The cells were then resuspended in 100 mL of medium which lacked a NO_3^- amendment and pelleted again in order to remove residual NO_3^- from the biomass. The cells were washed a second time in this very low NO_3^- medium and then the cells were resuspended in 50 mL of the very low NO_3^- medium. Assuming that 2 mL of residual liquid remained after decanting following each centrifugation step, these washing steps would result in decreasing the residual amended NO_3^- in the culture to < 0.003 μM.

Cell concentrations for the resuspended MIT0917 cells were determined by preparing 3 independent dilutions of each culture and counting cells using a Guava easyCyte 12HT Flow Cytometer (MilliporeSigma, Burlington, MA, USA). The washed cells were starved of N for 3

hours prior to initiation of the N pulse. Each culture was diluted to a final concentration of 1 x 10^{-8} cells mL^{-1} in duplicate 50 mL of very low NO_3^- medium. One of these duplicate cultures was spiked with 2 µM of sodium nitrate (to assess NO_2^- production at an environmentally relevant NO_3^- concentration) and the other duplicate culture was spiked with 2 µM of ammonium chloride (to serve as a control). Every 12 minutes over a time course of 2 hours, 4.5 mL of culture was removed from each tube and filtered through a 0.2 µm PES syringe filter into a 15 mL tube and then frozen at -20°C.

Within 24 hours, the samples were thawed and NO_2^- concentrations assessed using an AA3 HR continuous segmented flow analyzer (SEAL Analytical, Mequon, WI, USA), fitted with a 520 nm bandpass filter, by employing the G-384-08 method (SEAL Analytical) for the determination of NO_3^- and NO_2^- in water and seawater. The system wash was composed of artificial seawater (481 mM NaCl, 28 mM $MgSO_4$, 27 mM $MgCl_2$, 10 mM $CaCl_2$, and 9 mM KCl prepared using 18 megohm water). The color reagent, which reacts with NO_2^- to produce a pink-red azo dye, was composed of 1% sulfanilamide, 0.05% *N*-(1-naphthyl)ethylenediamine (NED), and 10% phosphoric acid prepared using 18 megohm water. Based on 15 independent measurements of zero calibrator samples and low concentration standards, the limit of blank (LOB; defined as the mean of blank samples plus 1.645 times the standard deviation of blank samples) of our assay was 9 nM NO_2^- and the limit of detection (LOD; defined as the LOB plus 1.645 times the standard deviation of a 15 nM NO_2^- standard) of our assay was 12 nM NO_2^-. The limit of quantitation of our assay was 30 nM NO_2^- (LOQ; defined as the lowest concentration of our standards that yields <10% coefficient of variation).

Table S1. *Prochlorococcus* and *Synechococcus* strains used in this study.

Strain	Genus	Subcluster/Clade	Inorganic N Assimilation	Original Reference	Rendered Axenic
MIT0915	*Prochlorococcus*	Clade LLI	NH_4^+, NO_2^-, NO_3^-	(9)	This Study
MIT0917	*Prochlorococcus*	Clade LLI	NH_4^+, NO_2^-, NO_3^-	(9)	This Study
MIT1214*	*Prochlorococcus*	Clade LLI	NH_4^+, NO_2^-	This Study	This Study
SB	*Prochlorococcus*	Clade HLII	NH_4^+, NO_2^-, NO_3^-	(16)	(1)
WH7803	*Synechococcus*	Subcluster 5.1B; Clade V	NH_4^+, NO_2^-, NO_3^-	(17)	(17)
WH8102	*Synechococcus*	Subcluster 5.1A; Clade III	NH_4^+, NO_2^-, NO_3^-	(17)	(17)

* A physiology study by Hawco et al. (18) was the first published instance of MIT1214, but as the original isolators of this strain, herein we report the methods and metadata for the isolation and genome sequencing of MIT1214.

Table S2. Inventory of nitrate and nitrite assimilation genes based on genomic data (6, 7) for the *Prochlorococcus* and *Synechococcus* strains used in this study.

	MIT0915	MIT0917	MIT1214	SB	WH7803	WH8102
Nitrite Transport and Reduction						
focA	●		●		●	
nirA	●	●	●	●	●	●
Nitrate Transport and Reduction						
napA	●	●		●	●	●
narB	●	●		●	●	●
Molybdopterin Cofactor Biosynthesis						
moaA	●	●		●	●	●
moaC	●	●		●	●	●
moaB	●	●		●	●	●
mobA	●	●		●	●	●
moeA	●	●		●	●	●
moaE	●	●		●	●	●
moaD	●	●		●	●	●
Genomic and Annotation Data						
NCBI GenBank Accession	CP114781	CP114784	CP114777	JNAS00000000	CT971583	BX548020
IMG Genome ID	2681812901	2681812859	2681813567	2606217677	640427149	637000314

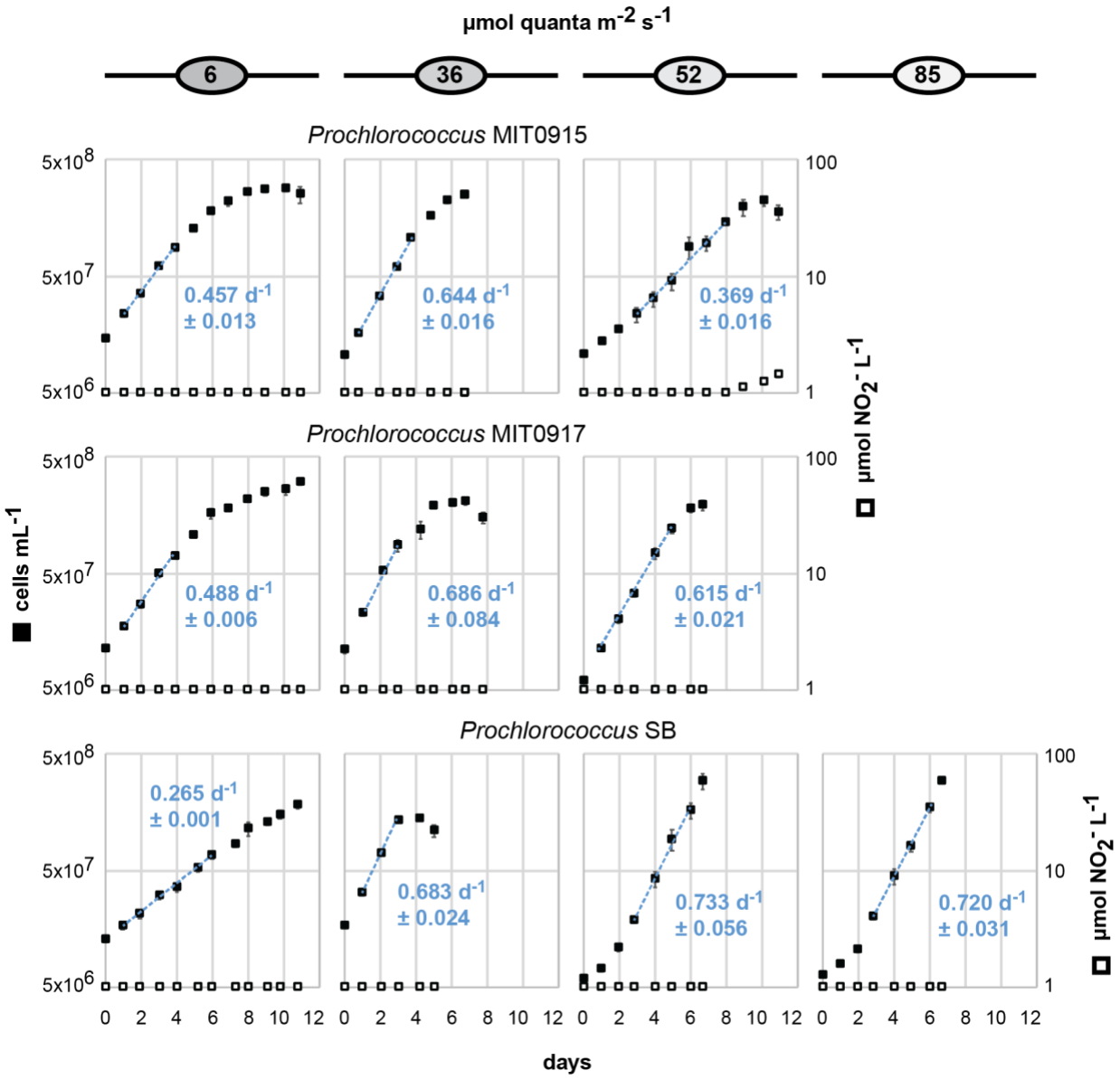

Fig. S1. Growth rates and extracellular NO_2^- concentrations for triplicate batch cultures of *Prochlorococcus* grown on NH_4^+ as the sole N source over a range of light intensities. Mean cell concentrations are denoted by closed black squares with error bars representing standard deviations. Growth rates (mean and standard deviation of µ for each replicate culture) are shown as blue text with the regression shown as a dashed blue line inclusive of the data points used to calculate growth rates. Mean NO_2^- concentrations are denoted by open squares with error bars representing standard deviations. NO_2^- concentrations below the dynamic range of the assay (< 1 µM NO_2^-) are plotted on the x-axis.

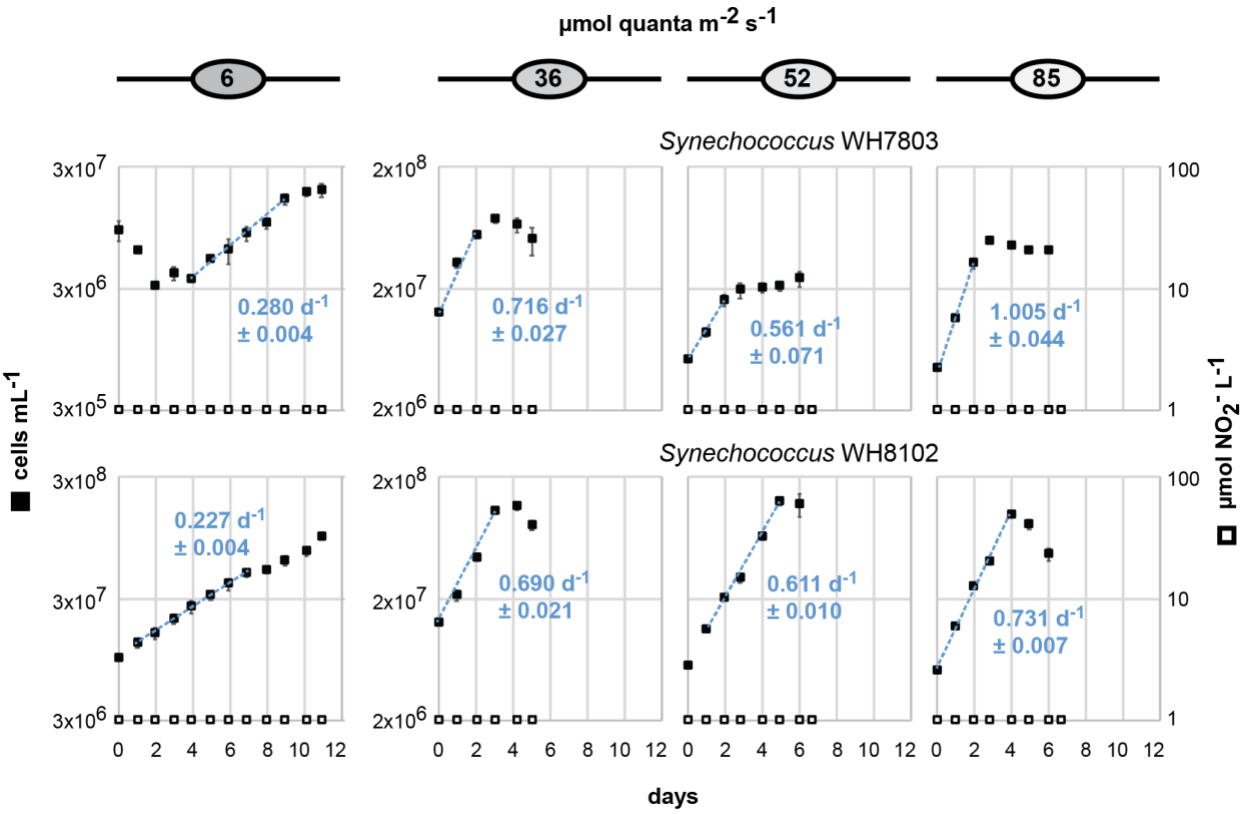

Fig. S2. Growth rates and extracellular NO_2^- concentrations for triplicate batch cultures of *Synechococcus* grown on NH_4^+ as the sole N source over a range of light intensities. Mean cell concentrations are denoted by closed black squares with error bars representing standard deviations. Growth rates (mean and standard deviation of µ for each replicate culture) are shown as blue text with the regression shown as a dashed blue line inclusive of the data points used to calculate growth rates. Note that the cell concentration range (left y-axis) on the plots for cultures grown at 6 µmol photons m^{-2} s^{-1} differs from the plots of cultures grown at higher light intensities. Mean NO_2^- concentrations are denoted by open squares with error bars representing standard deviations. NO_2^- concentrations below the dynamic range of the assay (< 1 µM NO_2^-) are plotted on the x-axis.

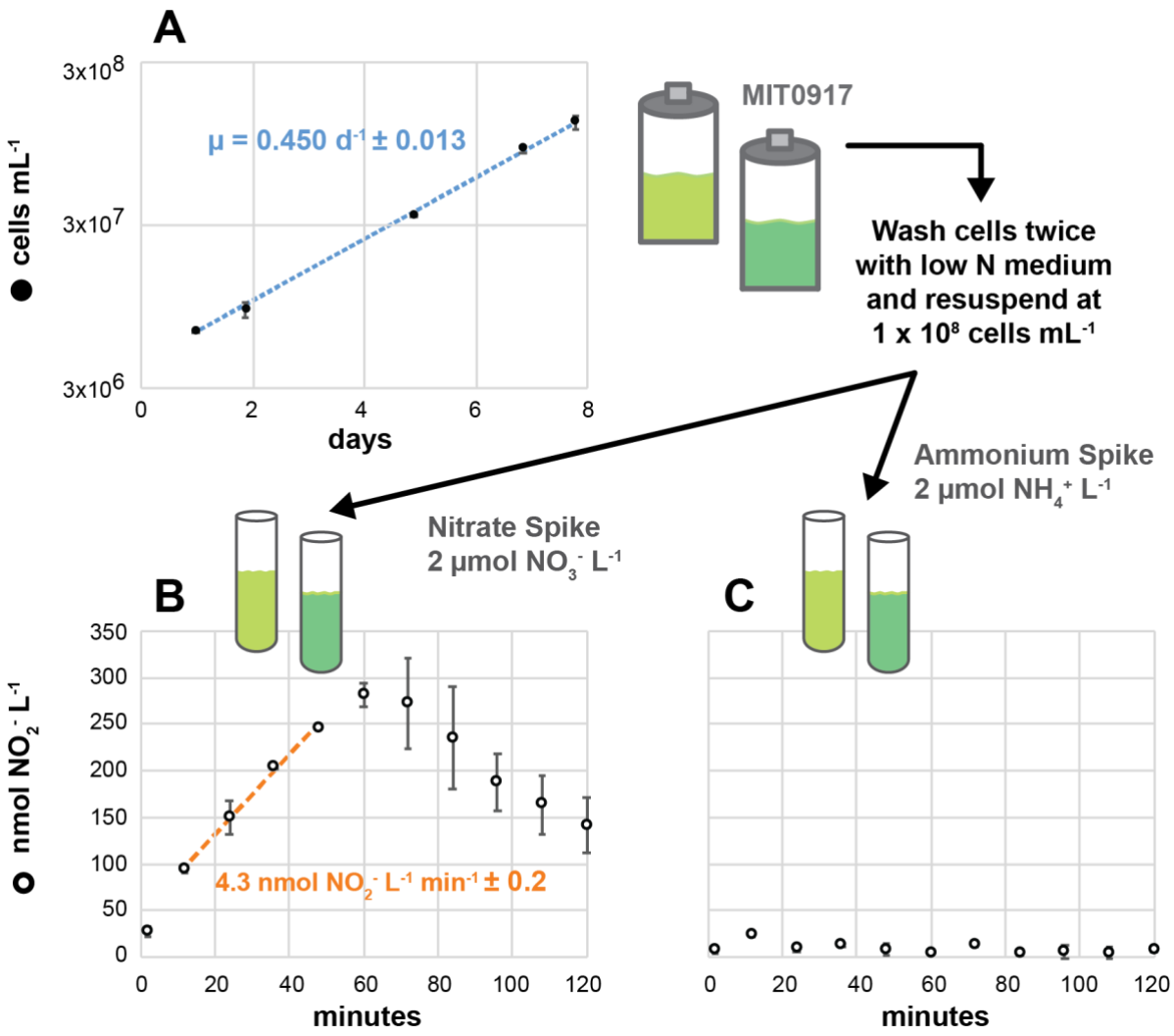

Fig. S3. NO_2^- production by *Prochlorococcus* MIT0917 in the presence of 2 μM NO_3^-. Mean cell concentrations for duplicate 250 mL cultures (A) are denoted by closed black circles with error bars representing standard deviations. Growth rate (mean and standard deviation of μ for each replicate culture) is shown as blue text with the regression shown as a dashed blue line inclusive of the data points used to calculate growth rates. Following the washing and resuspension of cells in low NO_3^- medium, NO_2^- concentrations were determined for duplicate cultures that were spiked with either 2 μM NO_3^- (B) or 2 μM NH_4^+ (C). NO_2^- concentrations are denoted by open black circles with error bars representing standard deviations. The bulk rate of NO_2^- accumulation (mean and standard deviation of the slope for each replicate culture spiked with 2 μM NO_3^-) is shown as orange text with the regression shown as a dashed orange line inclusive of the data points used to calculate the slope (B). The cell-specific NO_2^- production rate (accounting for a cell concentration of 1 x 10^8 cells mL^{-1}) was 6.1 x 10^{-8} (+/- 0.28 x 10^{-8}) nmol NO_2^- $cell^{-1}$ d^{-1}.

SUPPLEMENTARY REFERENCES

1. Berube PM, Biller SJ, Kent AG, Berta-Thompson JW, Roggensack SE, Roache-Johnson KH, Ackerman M, Moore LR, Meisel JD, Sher D, Thompson LR, Campbell L, Martiny AC, Chisholm SW. 2015. Physiology and evolution of nitrate acquisition in *Prochlorococcus*. ISME J 9:1195–1207.
2. Wilson K. 2001. Preparation of genomic DNA from bacteria. Curr Protoc Mol Biol 56:2.4.1–2. 4.2. https://doi.org/10.1002/0471142727.mb0204s56
3. Chin C-S, Alexander DH, Marks P, Klammer AA, Drake J, Heiner C, Clum A, Copeland A, Huddleston J, Eichler EE, Turner SW, Korlach J. 2013. Nonhybrid, finished microbial genome assemblies from long-read SMRT sequencing data. Nat Methods 10:563–569.
4. Markowitz VM, Chen I-MA, Palaniappan K, Chu K, Szeto E, Pillay M, Ratner A, Huang J, Woyke T, Huntemann M, Anderson I, Billis K, Varghese N, Mavromatis K, Pati A, Ivanova NN, Kyrpides NC. 2014. IMG 4 version of the integrated microbial genomes comparative analysis system. Nucleic Acids Res 42:D560–7.
5. Chen I-MA, Markowitz VM, Chu K, Palaniappan K, Szeto E, Pillay M, Ratner A, Huang J, Andersen E, Huntemann M, Varghese N, Hadjithomas M, Tennessen K, Nielsen T, Ivanova NN, Kyrpides NC. 2017. IMG/M: integrated genome and metagenome comparative data analysis system. Nucleic Acids Res 45:D507–D516.
6. Berube PM, Biller SJ, Hackl T, Hogle SL, Satinsky BM, Becker JW, Braakman R, Collins SB, Kelly L, Berta-Thompson J, Coe A, Bergauer K, Bouman HA, Browning TJ, De Corte D, Hassler C, Hulata Y, Jacquot JE, Maas EW, Reinthaler T, Sintes E, Yokokawa T, Lindell D, Stepanauskas R, Chisholm SW. 2018. Single cell genomes of *Prochlorococcus,*

Synechococcus, and sympatric microbes from diverse marine environments. Sci Data 5:180154.

7. Berube PM, Rasmussen A, Braakman R, Stepanauskas R, Chisholm SW. 2019. Emergence of trait variability through the lens of nitrogen assimilation in *Prochlorococcus*. eLife 8:e41043.
8. Kent AG, Baer SE, Mouginot C, Huang JS, Larkin AA, Lomas MW, Martiny AC. 2019. Parallel phylogeography of *Prochlorococcus* and *Synechococcus*. ISME J 13:430–441.
9. Berube PM, Coe A, Roggensack SE, Chisholm SW. 2016. Temporal dynamics of *Prochlorococcus* cells with the potential for nitrate assimilation in the subtropical Atlantic and Pacific oceans. Limnol Oceanogr 61:482–495.
10. Biller SJ, Berube PM, Dooley K, Williams M, Satinsky BM, Hackl T, Hogle SL, Coe A, Bergauer K, Bouman HA, Browning TJ, De Corte D, Hassler C, Hulston D, Jacquot JE, Maas EW, Reinthaler T, Sintes E, Yokokawa T, Chisholm SW. 2018. Marine microbial metagenomes sampled across space and time. Sci Data 5:180176.
11. Menzel P, Ng KL, Krogh A. 2016. Fast and sensitive taxonomic classification for metagenomics with Kaiju. Nat Commun 7:11257.
12. Becker JW, Hogle SL, Rosendo K, Chisholm SW. 2019. Co-culture and biogeography of *Prochlorococcus* and SAR11. ISME J 13:1506–1519.
13. Hogle SL. 2019. MARMICRODB database for taxonomic classification of (marine) metagenomes (Version 1.0.0) [Data set]. Zenodo https://doi.org/10.5281/zenodo.3520509
14. Letelier R. 2011. Nutrients from R/V Melville MV1015 in the South Pacific from Arica, Chile to Easter Island. from November to December 2010 (C-MORE project). Biological

and Chemical Oceanography Data Management Office (BCO-DMO). (Version 04 May 2011) Version Date 2011-05-04. http://lod.bco-dmo.org/id/dataset/3472

15. Moore LR, Coe A, Zinser ER, Saito MA, Sullivan MB, Lindell D, Frois-Moniz K, Waterbury J, Chisholm SW. 2007. Culturing the marine cyanobacterium *Prochlorococcus*. Limnol Oceanogr Meth 5:353–362.
16. Shimada A, Nishijima M, Maruyama T. 1995. Seasonal appearance of *Prochlorococcus* in Suruga Bay, Japan. J Oceanogr 51:289–300.
17. Waterbury JB, Watson SW, Valois FW, Franks DG. 1986. Biological and ecological characterization of the marine unicellular cyanobacterium *Synechococcus*, p 71–120. *In* Platt T, Li WKW (ed), Photosynthetic Picoplankton, Department of Fisheries and Oceans, Ottawa.
18. Hawco NJ, Fu F, Yang N, Hutchins DA, John SG. 2021. Independent iron and light limitation in a low-light-adapted *Prochlorococcus* from the deep chlorophyll maximum. ISME J 15:359–362.